

Downvalley fining of hillslope sediment in an alpine catchment: implications for downstream fining of sediment flux in mountain rivers

Leonard S. Sklar,^{1,2*}  Clifford S. Riebe,³  Jennifer Genetti,¹ Shirin Leclere¹ and Claire E. Lukens^{3,4}

¹ Department of Earth and Climate Sciences, San Francisco State University, San Francisco, CA USA

² Department of Geography, Planning, and Environment, Concordia University, Montreal, Canada

³ Department of Geology and Geophysics, University of Wyoming, Laramie, WY USA

⁴ Department of Geography, Victoria University of Wellington, Wellington, New Zealand

Received 2 October 2019; Revised 25 February 2020; Accepted 26 February 2020

*Correspondence to: Leonard S. Sklar, Department of Geography, Planning and Environment, Concordia University, Montreal, Canada. E-mail: leonard.sklar@concordia.ca
 This is an open access article under the terms of the Creative Commons Attribution License, which permits use, distribution and reproduction in any medium, provided the original work is properly cited.



ABSTRACT: The size distributions of sediment delivered from hillslopes to rivers profoundly influence river morphodynamics, including river incision into bedrock and the quality of aquatic habitat. Yet little is known about the factors that influence size distributions of sediment produced by weathering on hillslopes. We present results of a field study of hillslope sediment size distributions at Inyo Creek, a steep catchment in granitic bedrock of the Sierra Nevada, USA. Particles sampled near the base of hillslopes, adjacent to the trunk stream, show a pronounced decrease in sediment size with decreasing sample elevation across all but the coarsest size classes. Measured size distributions become increasingly bimodal with decreasing elevation, exhibiting a coarse, bouldery mode that does not change with elevation and a more abundant finer mode that shifts from cobbles at the highest elevations to gravel at mid elevations and finally to sand at low elevations. We interpret these altitudinal variations in hillslope sediment size to reflect changes in physical, chemical, and biological weathering that can be explained by the catchment's strong altitudinal gradients in topography, climate, and vegetation cover. Because elevation and travel distance to the outlet are closely coupled, the altitudinal trends in sediment size produce a systematic decrease in sediment size along hillslopes parallel to the trunk stream. We refer to this phenomenon as 'downvalley fining.' Forward modeling shows that downvalley fining of hillslope sediment is necessary for downstream fining of the long-term average flux of coarse sediment in mountain landscapes where hillslopes and channels are coupled and long-term net sediment deposition is negligible. The model also shows that abrasion plays a secondary role in downstream fining of coarse sediment flux but plays a dominant role in partitioning between the bedload and suspended load. Patterns observed at Inyo Creek may be widespread in mountain ranges around the world. © 2020 The Authors. Earth Surface Processes and Landforms published by John Wiley & Sons Ltd.

KEYWORDS: downvalley fining; sediment size distributions; river bedload; physical weathering; chemical weathering; landscape evolution

Introduction

Most of Earth's land surface is covered by regolith, a blanket of particles composed primarily of rock and mineral fragments originally derived from bedrock underlying hillslopes. The sizes of these bedrock-derived particles can span more than six orders of magnitude, from boulders to clay, reflecting the wide range of lithologic, climatic, and geomorphic environments where particles are first eroded from bedrock and then weathered during transport downslope. Particle size, in turn, fundamentally influences the processes of erosion, weathering, and transport that shape the morphology of both hillslopes and river channels. On hillslopes, regolith particle size distributions influence topographic slope (Granger et al., 2001), water through-flow (Lohse and Dietrich, 2005), chemical weathering

rates (Yoo et al., 2011), and nutrient supply to ecosystems (Chadwick et al., 1999). Once particles enter the river, their sizes affect channel slope (Howard, 1980; Sklar and Dietrich, 2006; Finnegan et al., 2017), bedrock river incision (Sklar and Dietrich, 2004; Turowski et al., 2015), and the type and quality of aquatic habitat (Riebe et al., 2014; Wohl et al., 2015). Despite the importance of particle size in landscape dynamics (Callahan et al., 2019), little is known about what controls the initial sizes of sediment produced on hillslopes or how sediment size distributions evolve as particles are transported downslope and delivered to channels (Sklar et al., 2017).

Addressing these knowledge gaps is important for understanding patterns of sediment size variation through river networks, including the widely recognized downstream fining of bed material (Pizzuto, 1995; Blom et al., 2016). Downstream

fining in depositional landscapes is commonly explained as the result of preferential transport of smaller particles (Paola et al., 1992; Ferguson et al., 1996; Fedele and Paola, 2007), while particle abrasion is thought to dominate in erosional landscapes, because little accommodation space exists to store large volumes of coarse sediment (Kodama, 1994; Miller et al., 2014). However, in the uplands of erosional landscapes, where hillslopes and channels are closely coupled, downstream fining could also result from downvalley fining of sediment supplied by hillslopes to channels (Attal and Lavé, 2006; Sklar et al., 2006). (Here, and throughout this manuscript, we use 'downvalley' to refer to trends in hillslope attributes running parallel to the trunk stream; 'downslope' to refer to trends running perpendicular to hillslope contour lines; and 'downstream' to refer to trends within the channel.) For a given reach of river, sediment supplied from adjacent hillslopes can contribute significantly to the long-term average flux of sediment too coarse to be transported in suspension (Sklar et al., 2006). This material moves instead as bedload and provides the particles from which the bed is formed. Local hillslope supply is particularly important where particles are easily abraded, because mass lost by abrasion to sand and silt reduces the contribution of upstream sources to the local bed sediment size distribution (Sklar et al., 2006). However, downvalley fining of hillslope sediment only occurs where there are downvalley variations in the factors that control sediment production and weathering on hillslopes.

Many previous studies have sought to quantify how physical and chemical erosion are influenced by topography and climate, but few have explored the factors that influence the size distributions of sediment produced on slopes, and none to our knowledge have explored how size distributions vary downvalley. In a recently developed theoretical framework, the sizes of sediment produced on hillslopes and supplied to channels are modeled in a two step process (Sklar et al., 2017). The first step is to characterize the initial, latent size distribution of the blocks within the unweathered bedrock, which should depend on the distributions of spacings between fractures and beds, or the sizes of clasts cemented within sedimentary rock. The second step is to predict how the initial size distribution is transformed *en route* to the channel by chemical and physical weathering. The extent of weathering, and thus size reduction, is modeled as a function of three factors: lithology, represented by the fraction of soluble minerals; climate, characterized by mean annual temperature and precipitation; and erosion rate, which governs particle residence times in the weathering engine. Most of these factors can vary systematically with elevation across a catchment, thereby creating altitudinal gradients in hillslope sediment size. Because elevation is correlated with distance downstream, altitudinal gradients in hillslope sediment size could lead to downvalley fining of sediment supply to channels.

Available data, though limited, suggest that hillslope sediment size may commonly vary with elevation due to gradients in precipitation (Marshall and Sklar, 2012), hillslope steepness (Attal et al., 2015), and erosion rate (Whittaker et al., 2010). For example, cosmogenic nuclides and detrital (U-Th)/He ages from two sediment sizes sampled from Inyo Creek, in the Sierra Nevada, California, reveal that coarse gravel is preferentially produced at higher elevations, while fine gravel and sand are preferentially produced at lower elevations (Riebe et al., 2015; Lukens et al., 2016, 2020). Higher elevations in this catchment are also colder, steeper, less vegetated, and are eroding more rapidly (Riebe et al., 2015). Together, these observations suggest an overall fining in sediment size with decreasing elevation across the Inyo Creek catchment, due to variations in the climatic and geomorphic factors that influence hillslope sediment size.

Although available data from Inyo Creek suggest that hillslope sediment size can vary systematically at the catchment scale, they also raise new questions. Does the pattern extend to other size classes besides the coarse gravel and finer sediment? If so, how sharp is the gradient in particle size with elevation? Is the trend continuous or are there thresholds due to shifts in the dominant sediment production process? Is this the signal of climate-driven variations in hillslope weathering, or could it instead reflect an altitudinal trend in the latent size distribution set by fracture spacings in bedrock?

To answer these questions, we returned to Inyo Creek to investigate sediment production, weathering, and transport on the hillslopes that produce the sediment that is ultimately delivered to the sampling site at the catchment outlet. We measured size distributions of surface sediment along an altitudinal gradient through the accessible portion of the catchment. We also measured bedrock fracture spacing and collected evidence of processes responsible for sediment production on hillslopes. Our results are consistent with an exponential reduction in surface particle size with decreasing elevation and a spatially uniform pattern in fracture spacing. This suggests that spatial variations in weathering are largely responsible for downvalley fining of hillslope sediment in this landscape.

Inyo Creek field site

The Inyo Creek catchment is incised into the eastern escarpment of the Sierra Nevada, California, USA (Figure 1a). It spans nearly 2 km of vertical relief over less than 5 km of map distance (Figure 1b), from Lone Pine Peak, the highest point at 3950 m elevation, to the outlet at 2050 m elevation, the apex of a debris fan along the mountain front. Near the outlet, the channel crosses the Sierra Nevada Frontal Fault, an active normal fault with vertical slip rates that locally range from 0.1 to 0.3 mm yr⁻¹ (Le et al., 2007). Bedrock underlying the catchment includes three Late Cretaceous plutons: the Whitney, Paradise, and Lone Pine granodiorites, which vary little in mineral composition (Hirt, 2007). The catchment has little sediment accommodation space because it remained unglaciated throughout the Pleistocene (Brocklehurst and Whipple, 2004; Stock et al., 2006) and because steep hillslope and channel gradients promote rapid transport of sediment to the outlet.

Many of the factors that should influence sediment size, such as local climate, hillslope gradient, erosion rate, and land cover, vary strongly with elevation at Inyo Creek (Riebe et al., 2015). This makes the catchment an ideal site for observing downvalley fining of hillslope sediment in the field. Along its 2 km elevation gradient, we expected to see a shift from dominantly physical weathering at high elevations to chemical weathering at low elevations (Riebe et al., 2015). For example, mean annual temperature, which regulates chemical weathering (Riebe et al., 2004), warms by 11 °C, from -1 °C at the peak to 10 °C at the outlet (PRISM Climate Group, 2014). Mean annual precipitation, which provides water for both frost cracking (Marshall et al., 2015) and dissolution reactions (Lebedeva and Brantley, 2013), decreases from 710 mm yr⁻¹ at the highest elevation to 290 mm yr⁻¹ at the lowest. Erosion rates, which control particle residence times in the weathering zone, appear to decrease by an order of magnitude, from > 1.0 mm yr⁻¹ at the top to < 0.1 mm yr⁻¹ at the bottom, according to a coupled analysis of cosmogenic nuclides and (U-Th)/He ages in sediment collected from the outlet (Riebe et al., 2015). Meanwhile, hillslope gradients are remarkably steep throughout the catchment. The upper 50% of the catchment (above 2800 m) has an average hillslope angle of 42° ± 9° (mean ±

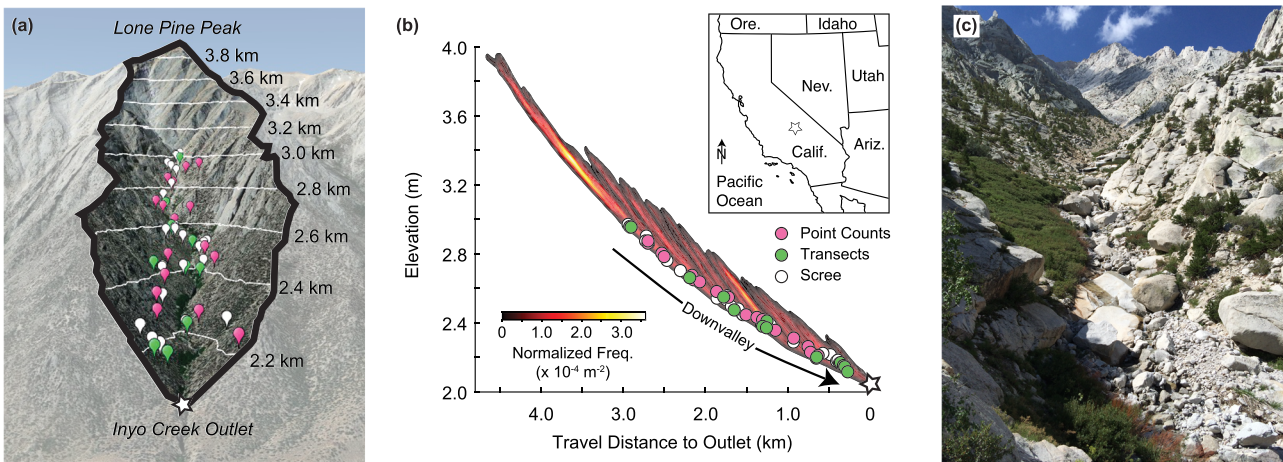


Figure 1. Inyo Creek field site and sampling locations in California, USA (inset of panel b). (a) Google Earth view of Sierra Nevada escarpment, showing Inyo Creek catchment, 200-m elevation contours, and locations of surface point counts (pink), transects (green), and scree slope measurements (white). (b) Profile view of the joint distribution of catchment elevation and travel distance to the outlet for every pixel in the digital elevation model (DEM), showing strong correlation between elevation and distance downvalley for sampling locations; measurement locations were selected to capture particle size distributions representative of sediment supply to channel along valley axis. (c) View upstream from ~2600-m elevation, showing Inyo Creek channel. [Colour figure can be viewed at wileyonlinelibrary.com]

standard deviation); the lower 50%, in contrast, has an average slope of 27° (Figure 2a), suggesting a transition from threshold to non-threshold slopes (Clarke and Burbank, 2010).

The extent and character of regolith also varies systematically with elevation. In an initial field reconnaissance, we traversed as much of the catchment as we could safely access without climbing gear. We found that regolith is largely absent and bare bedrock dominates land cover at the highest elevations (Figure 2b), where erosion rates are fastest and temperatures are coldest. In contrast, the warmer and slower eroding lower-elevation hillslopes are mantled with a bimodal mix of sand and widely scattered boulders and bedrock outcrops. Gravel- and cobble-sized particles are largely absent at the lower elevations (Figure 2d), which made it impossible to find clasts for cairns to mark our route. Between the upper and lower elevation extremes, at middle elevation hillslopes, we found three types of land cover: large expanses covered by poorly-sorted mixtures of coarse particles ranging from sand to boulders (Figure 2c); well-sorted angle-of-repose slopes of scree and talus that extend tens to hundreds of meters upslope from the valley axis (Figure 2g); and outcrops of bare bedrock (Figure 2e, f).

Sediment production and transport processes also appear to vary with elevation across the catchment. On the high-elevation bedrock slopes, we found evidence of recent bedrock landslides that traveled as rocky debris flows to the lower catchment and out onto the fan (Arabnia and Sklar, 2016). In contrast, near the catchment outlet, evidence of gruss production is ubiquitous: crumbling boulders and bedrock outcrops are surrounded by aprons of disaggregated mineral crystals. Through the middle elevations we found evidence of both rock fall and gruss production, along with intensely fractured rock suggestive of frost cracking. The channel qualitatively reflects this pattern, with bare bedrock above 3000 m elevation, a boulder-dominated reach at middle elevations (Figure 1c), and a step-pool morphology near the outlet where slopes are gentler (Figure 1b). Overall, these qualitative observations imply a systematic altitudinal gradient in dominant sediment production processes and particle size, shifting from physical weathering mechanisms and coarser sediment at higher elevations, to chemical weathering and a bimodal distribution of both finer sediment and boulders at lower elevations.

Methods

To quantify variations in hillslope particle size across the elevation gradient, we used four methods: point counts, bulk samples, transects, and gridded point counts using digital images (i.e. photo sieving). We also measured bedrock fracture spacing to determine whether there is any spatial variation in initial particle size. Our measurements quantify size distributions of particles at the surface. Systematic subsurface sampling was not feasible, except at the lowest elevations, where we dug several pits up to 1 m depth in the grassy soil and found no apparent difference between surface and subsurface particle size. At higher elevations, the frequent occurrence of bedrock outcrops suggests that the thickness of sediment accumulations is similar in scale to the diameter of the largest particles at the surface (Figures 2e, f).

Point counts

We used point counts to measure surface particle size at 17 locations ranging in elevation from 2875 m, the highest elevation safely accessible without climbing gear, down to 2212 m, on hillslopes just above the catchment outlet at the fan apex (Figure 1). Sites were selected using a stratified-random sampling approach to avoid bias while also covering the full elevation range. To obtain a sample set representative of the range of sediment production processes, we used geographic information system (GIS) analysis to divide the catchment into geomorphic landscape units (GLUs), which are polygons with shared topographic and climatic attributes (Booth et al., 2014). We grouped polygons into three types, which we hypothesized would produce particles with relatively large, intermediate, and small sizes, respectively. We assumed that large sizes are associated with steep hillslope gradients, south-facing aspects, low surface biomass, and favorable conditions for frost cracking. For each GLU type, we selected six polygons spanning the accessible elevation range, and then randomly assigned sampling coordinates within each polygon. In the field, we used a global positioning system (GPS) receiver to locate the assigned coordinates, and conducted the point counts at those locations, sampling sediment along a measuring tape that we stretched along multiple, 15 m spoke-like lines radiating from a central point

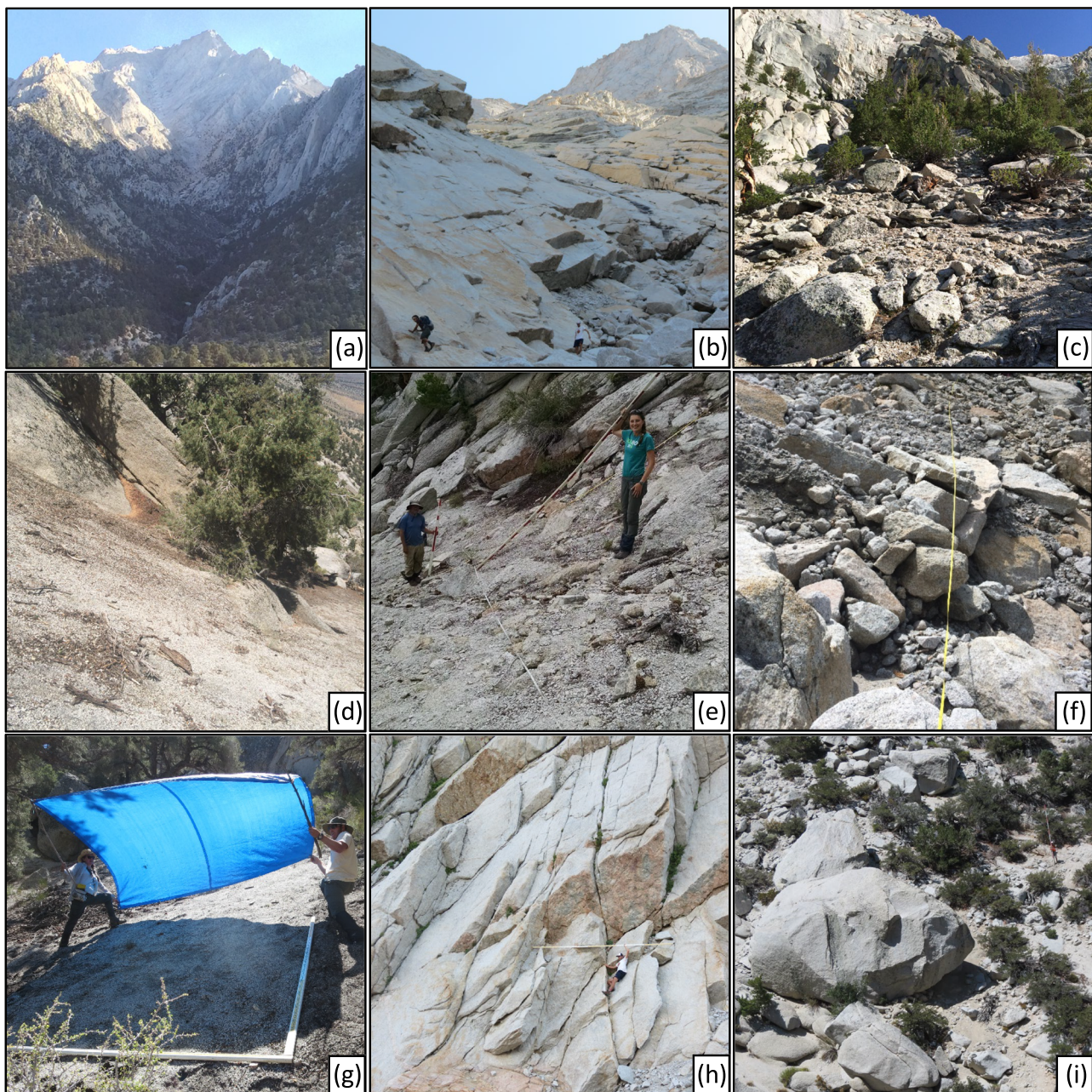


Figure 2. Field photographs. (a) View of Inyo Creek catchment, with fan apex at bottom of photograph. (b) Bare bedrock dominates at higher elevations (in this case ~3000 m). (c) Middle elevations (in this case 2412 m) are characterized by wide particle size distributions and bedrock outcrops. Boulder in foreground has ~1 m diameter. (d) Ground surface at lower elevations (2260 m) dominated by gruss, sand, boulders and bedrock. (e) Point count sampling at 2582 m elevation. (f) Tape transect sampling location at 2660 m elevation. (g) Photo-sieve sampling location at 2240 m elevation. Tarp was used to shade sample area and thus control image contrast. (h) *In situ* measurement of bedrock fracture spacing, at 2970 m elevation. (i) Large boulders (> 5 m diameter, note person in upper right of photograph for scale) shed from steep bedrock slopes above (elevation = 2700 m). [Colour figure can be viewed at wileyonlinelibrary.com]

(Figure 2e). Beginning with a line along the steepest descent, we spaced the lines in eight angular increments of 45° and thus encompassed a circular area of approximately 100 m² at each sampling site. At each 50 cm increment along the tape, we measured the intermediate ('b') axis diameters of particles with diameter (D) > 5 mm. Otherwise points were categorized as '< 5 mm' or 'bare bedrock' as appropriate.

Bulk sampling

To quantify the fine tail of the point-count-based size distributions, we collected bulk samples at 20 points where the surface was categorized as < 5 mm, both within the point-count

locations and at other locations across the elevation range. Bulk samples were collected with a trowel to a depth of 10 cm; sample volumes exceeded 10⁻³ m³ and thus were greater than minimum sampling requirements for particles with $D < 5$ mm (Marshall and Sklar, 2012). Samples were transported to the laboratory where any organic material was removed by hand. After oven drying the samples, we measured their particle size distributions by first weighing any individual particles > 5 mm by hand to avoid mechanical disaggregation and then sieving the remaining finer material in ½ phi increments down to 0.5 mm. For the individual particles we calculated *b*-axis diameter assuming nominally spherical particles with a density of 2500 kg m⁻³. Because the size distributions of the bulk samples showed no trend with elevation, we used

a catchment wide mean distribution from the bulk sampling to represent the fine tail of the point-count-based size distributions. We did this by weighting the proportions in each increment of the bulk samples by the fraction < 5 mm observed in the point counts.

Transects

To quantify surface particle size distributions at a larger scale we created transects by stretching 100 m tapes across areas within uniform GLU polygons (Figure 2f). We then divided the transect into continuous segments according to the dominant particle size class within each segment, using four size bins: fine ($D < 5$ mm), gravel ($5 < D < 64$ mm), cobble ($64 < D < 128$ mm), and boulder ($D > 128$ mm), with an additional category for bare bedrock. We collected transect data at 12 locations ranging in elevation from 2145 to 2950 m (Figure 1).

Scree slopes

To characterize the size distributions of the scree-dominated slopes, we used point counts taken from scaled digital images of surface material. Digital images were acquired on angle-of-repose slopes of well-sorted material, across 25 elevations ranging from 2177 to 2972 m. Coordinates for scree samples were selected from aerial photographs, where they stand out as uniform light-colored strips oriented sub-perpendicular to the valley axis. Once at the selected coordinates, we determined the center points of the samples by blindly tossing a weighted flag backwards, toward the middle of the scree slope. At each center point, we placed stadia rods perpendicular and parallel to the path of steepest descent and photographed the surface material from 2 m above. The camera was mounted on a gimbal and pole to avoid disturbing the sampling area. To maintain uniform lighting conditions across the images, we shaded the sampling area using hand-held tarp canopies (Figure 2g). After the images were orthorectified, particle size was measured at 100 grid nodes, assuming that the shorter visible axis represents the intermediate *b*-axis (Ibbeken and Schleyer, 1986). The minimum detectable size was 1 mm.

Fracture spacing measurements

Fracture spacing in bedrock near the Earth's surface is a first-order control on the size distribution of particles that have been converted from bedrock to regolith on hillslopes (Roy et al., 2016; Sklar et al., 2017; DiBiase et al., 2018; Neely et al., 2019; Scott and Wohl, 2019). To test for spatial gradients in the size of fracture-bound bedrock blocks, we measured fracture spacing using several approaches. First, at the bedrock outcrops that can be found scattered across regolith-dominated slopes, we placed stadia rods perpendicular to parallel fractures to measure the characteristic size of individual blocks. We also measured fracture spacing at the base of steep, bare-bedrock slopes (Figure 2h), focusing on locations upslope of the point count sampling sites to acquire a representative sample across the accessible elevation gradient. In sum we obtained 166 *in situ* measurements of fracture spacing at elevations ranging from 2217 to 2976 m. Because steep slopes render most of the upper catchment inaccessible, we also measured the spacing of fractures visible in scaled, ortho-rectified aerial photographs. This was done by drawing transects perpendicular to the valley axis, and measuring the distance

between fractures along the transect, irrespective of the orientation of the fractures. At each point where fractures crossed the transect, we estimated the corresponding elevation by overlaying the aerial photographs on a 10-m digital elevation model (DEM). We obtained 426 aerial photographs based measurements of fracture spacing at elevations ranging from 2200 to 3369 m.

Results

Our particle size analyses reveal a strong altitudinal, and thus downvalley decrease in mean hillslope sediment size at Inyo Creek. The decrease occurs across the entire sampled elevation range and is evident in results from each of the measurement techniques. As elaborated later, the decrease in mean sediment size reflects a gradual shift from a coarse cobble- and boulder-dominated distribution at upper sampling sites to a bimodal distribution of sand and boulders near the catchment outlet. Data reported later and displayed in accompanying figures are provided in the Supporting Information, Data S1, available with the online version of this article.

Point count data

The point count data show that the range of particle sizes spans more than four orders of magnitude across the sampling sites, varying from 0.1 mm to more than 3 m in *b*-axis diameter (Figure 3). Cumulative distribution functions (CDFs) of the point count data show that particle size decreases systematically with elevation and therefore distance from the highest sampling points (Figure 3a). This downvalley fining is quantified in altitudinal trends of the proportions of sediment that occur in different size classes (Figure 3b–f). For example, the proportions of sediment in the < 2 mm and 2–8 mm size classes each exhibits a statistically significant ($p < 0.05$) linear increase with decreasing elevation ($p = 0.003$ and 0.0009 respectively). This is compensated by a statistically significant altitudinal (and thus downvalley) decrease in the proportion of sediment in the 8–32 mm and 32–128 mm size classes. Conversely, the proportion in the > 128 mm size class shows no significant trend ($p = 0.098$) with elevation (all regression statistics are listed in Table 1).

The observed trends in proportions of the different size classes are reflected in altitudinal variations in the percentiles of the CDFs (Figure 3g–i). For example, the central tendency of the particle size distribution, defined here as the median particle size (or D_{50}), decreases exponentially with decreasing elevation from 30 mm to 3 mm (Figure 3h). The 16th percentile values of the particle size distributions (D_{16}) likewise show a statistically significant exponential decrease from the highest to lowest sampling points (Figure 3g). In contrast, the 84th percentile values of the particle size distributions (D_{84}) do not show a statistically significant altitudinal trend (Figure 3i). Together, the CDFs (Figure 3a) and particle size statistics indicate that downvalley fining in hillslope sediment occurs due to systematic trends in the fine and intermediate sediment sizes (Figure 3b–e, g, h), despite the relatively uniform fractional amount of coarse sediment (Figure 3f, i) at each site.

Comparison of point counts and transects

Similar altitudinal trends are evident in results from the transect sampling sites (Figure 4). As elevation declines from 3.0 km to 2.2 km, the abundance of sediment with $D <$

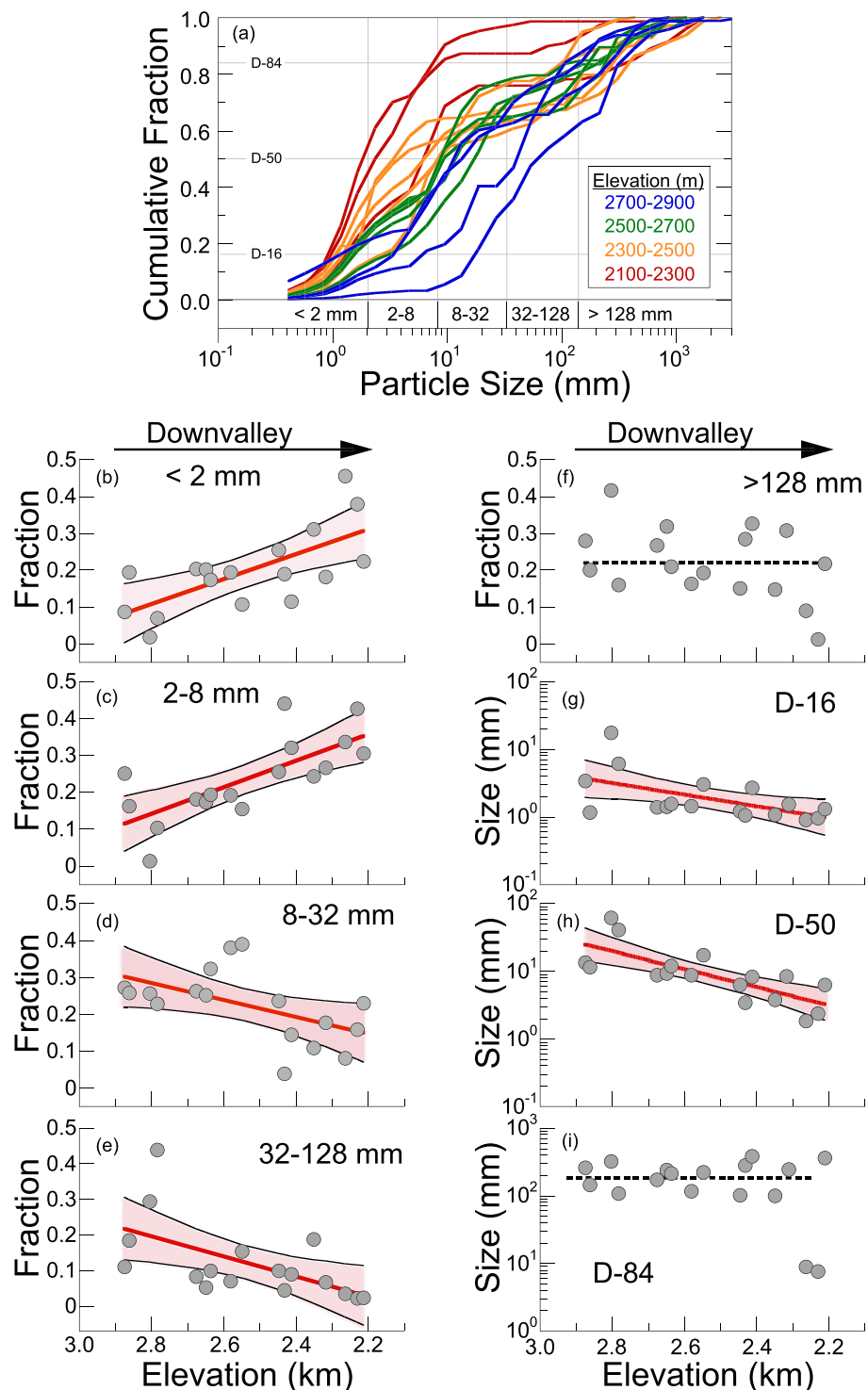


Figure 3. Point count results. (a) Cumulative particle size distributions for 17 surface point count sampling locations, colors vary from warm for low elevations to cool for high elevations. (b–f) Variation with elevation of sediment fraction within five size-class bins; bin boundaries indicated by vertical lines in (a). (g–i) Variation with elevation of three size-distribution quantiles, indicated by horizontal lines in (a). Statistically significant regression lines are indicated in red, with 95% confidence curves; where correlation is not significant, mean value is indicated by dashed line. Regression statistics are listed in Table 1. Significant downvalley fining is shown by decreases in coarser sediment fractions, and corresponding downvalley increases in finer sediment fractions, as well as by exponential decreases in the 16th and 50th quantiles. Only the coarsest size class (> 128 mm) and 84th quantile show no significant variation with elevation. [Colour figure can be viewed at wileyonlinelibrary.com]

5 mm increases steadily as the fraction in the gravel and cobble size classes decreases. Analyses of regression slopes of sediment abundance against elevation show no statistically significant differences between the altitudinal trends in point counts and transects for the < 5 mm, gravel (5–64 mm), and cobble (64–256 mm) size classes. In addition, neither measurement type shows a significant altitudinal trend in boulder

(> 256 mm) abundance. The consistency between the point count and transect data indicates that our ability to detect the downvalley trends in sediment size is not strongly affected by sampling technique. It also indicates that we can combine the point count and transect data together for improved spatial resolution of downvalley variations in particle size distribution (Figure 4).

Table 1. Regression statistics for altitudinal trends in particle size distributions.

Panel	Dependent variable	Fit type	Intercept	Slope	p	r^2
<i>Figure 3 – Point counts (n=17)</i>						
b	Fraction < 2 mm	Linear	0.21 ± 0.02	-0.34 ± 0.09	0.0025	0.47
c	Fraction $2 < D < 8$ mm	Linear	0.25 ± 0.02	-0.36 ± 0.09	0.0009	0.53
d	Fraction $8 < D < 32$ mm	Linear	0.22 ± 0.02	0.23 ± 0.10	0.029	0.28
e	Fraction $32 < D < 128$ mm	Linear	0.11 ± 0.02	0.28 ± 0.10	0.014	0.34
f	<i>Fraction D > 128</i>	<i>Linear</i>	<i>0.21 ± 0.02</i>	<i>0.18 ± 0.10</i>	<i>0.098</i>	<i>0.17</i>
g	D_{16} (log)	Exponential	0.24 ± 0.08	0.86 ± 0.32	0.018	0.32
h	D_{50} (log)	Exponential	0.89 ± 0.08	1.33 ± 0.30	0.0004	0.57
i	D_{84} (log)	Exponential	2.10 ± 0.16	0.89 ± 0.53	0.11	0.16
<i>Figure 4 – Point counts and transects (n=29)</i>						
a	Percentage < 5 mm	Linear	40.6 ± 3.2	-0.064 ± 0.013	< 0.0001	0.46
b	Percentage gravel	Linear	24.4 ± 2.3	0.037 ± 0.009	0.0005	0.37
c	Percentage cobble	Linear	11.0 ± 1.3	0.013 ± 0.005	0.019	0.19
d	Percentage boulder	Linear	23.9 ± 2.3	0.013 ± 0.009	0.18	0.07
<i>Figure 6 – Bimodal fit parameters (n = 17)</i>						
a	Fine mode mean (mm)	Exponential	5.5 ± 1.2	1.27 ± 0.32	0.0009	0.51
b	Fine mode standard deviation (log)	Linear	0.48 ± 0.02	0.25 ± 0.11	0.038	0.26
c	Coarse mode mean (mm)	Exponential	2.51 ± 0.07	0.05 ± 0.31	0.87	< 0.01
d	Coarse mode standard deviation (log)	Linear	0.33 ± 0.03	-0.13 ± 0.13	0.34	0.06
e	Fine fraction	Linear	0.75 ± 0.03	-0.03 ± 0.13	0.84	< 0.01
<i>Figure 8 – Scree samples (n=25)</i>						
b	D_{16} (mm)	Exponential	0.65 ± 0.04	0.42 ± 0.16	0.018	0.22
c	D_{50} (mm)	Exponential	0.95 ± 0.26	0.80 ± 0.14	< 0.0001	0.60
d	D_{84} (mm)	Exponential	1.30 ± 0.38	1.02 ± 0.14	< 0.0001	0.70
e	Geometric standard deviation	Linear	0.33 ± 0.02	0.30 ± 0.08	0.0009	0.39

All regression parameters based on linear ordinary least-squares regression against elevation, represented by $Z - Z^*$ where Z is sample elevation in meters and Z^* is a reference elevation equal to 2500 m (roughly the middle of the data range spanned in each regression).

Fit type indicates whether regressions were fit to linear or log-transformed (exponential) dependent variable data.

Intercept values correspond to the height of the regression at the reference elevation (2500 m) in our regressions.

Data sets in which the confidence level was less than 95% ($p > 0.05$) are indicated by italic typeface; for these cases we display the mean of the dependent variable as a horizontal line in the figures. Uncertainty for all parameter estimates is expressed as standard error.

Bimodal distributions of particle size

The absence of downvalley trends in the coarsest size fractions, despite clear trends in the finer size classes, suggests the sediment size distributions have two distinct modes and that the finer mode varies across the catchment while the coarser mode is more spatially uniform. Inspection of the point count probability distribution functions (PDFs) confirms this expectation (Figure 5). At the highest elevation sampling locations, the distributions are strongly bimodal, with a fine mode centered on coarse gravel and a coarse mode centered on coarse cobbles and boulders (Figure 5a–d). At lower elevation sites, farther downvalley, the fine mode appears to shift to smaller particle sizes while the coarse mode remains static, consisting of cobbles and boulders (e.g. Figure 5j–n).

Recognizing that the distributions are strongly bimodal, we modeled them as weighted sums of two log-normal distributions in a least-squares optimization routine that finds the best-fit weighting factor as well as the mean and standard deviation of each mode. The best-fit models are plotted with the measured distributions in Figure 5. If the coarse mode is spatially uniform and the fine mode accounts for the observed downvalley decrease in D_{50} (Figure 3h), we would only see downvalley trends in the modeled mean of the fine mode. This prediction is confirmed in Figure 6, which shows a statistically significant downvalley decrease in the best-fit fine-mode mean (Figure 6a), but no significant variation in the coarse mode mean (Figure 6c). The model fits also show a significant altitudinal decrease in the standard-deviation of the fine-mode size distribution (Figure 6b), but no significant variation in the standard-deviation of the coarse-mode (Figure 6d). In addition, the fraction of sediment in the fine mode (i.e. the modeled weighting factor) averages 0.75 ± 0.03 (mean \pm standard error)

and shows no significant trend with elevation and thus distance downstream (Figure 6e). Because the fine mode includes an average of three quarters of the distributions (and thus dominates them), the order-of-magnitude variation in the fine-mode mean (Figure 6a) readily accounts for the observed decrease in the overall median particle size (Figure 3h). We also note that the downvalley narrowing of the fine mode reflects the observed loss of particles in the 32–128 mm size class (Figure 3e).

Fracture spacing distributions

The observed downvalley variations in the fine mode of the particle size distributions raises the question of whether they are driven in part by a downvalley trend in bedrock fracture spacing. Although fracture spacing spans more than two orders of magnitude in range (Figure 7), it does not correlate strongly with elevation in either the *in situ* or aerial photograph-based measurements ($r^2 = 0.025$ and 0.027, respectively). This indicates that fracture spacing does not vary systematically with downvalley distance across our study sites. The aerial photograph analysis yields fracture spacings that are 3.9 times higher on average than the fracture spacings from the field-based measurements. This likely reflects biases from two sources: resolution of the aerial photographs (which is too low to detect spacings less than ~0.5 m); and length of the stadia rod in the field (which is too short to measure spacings greater than ~4 m). However, these biases do not inhibit our ability to detect trends (if present) with elevation, given the wide range in spacings that can be measured using each technique. When aggregated across all sites, the fracture spacing distribution from the field-based measurements is only slightly coarser than the spatially averaged coarse mode of the particle size distributions.

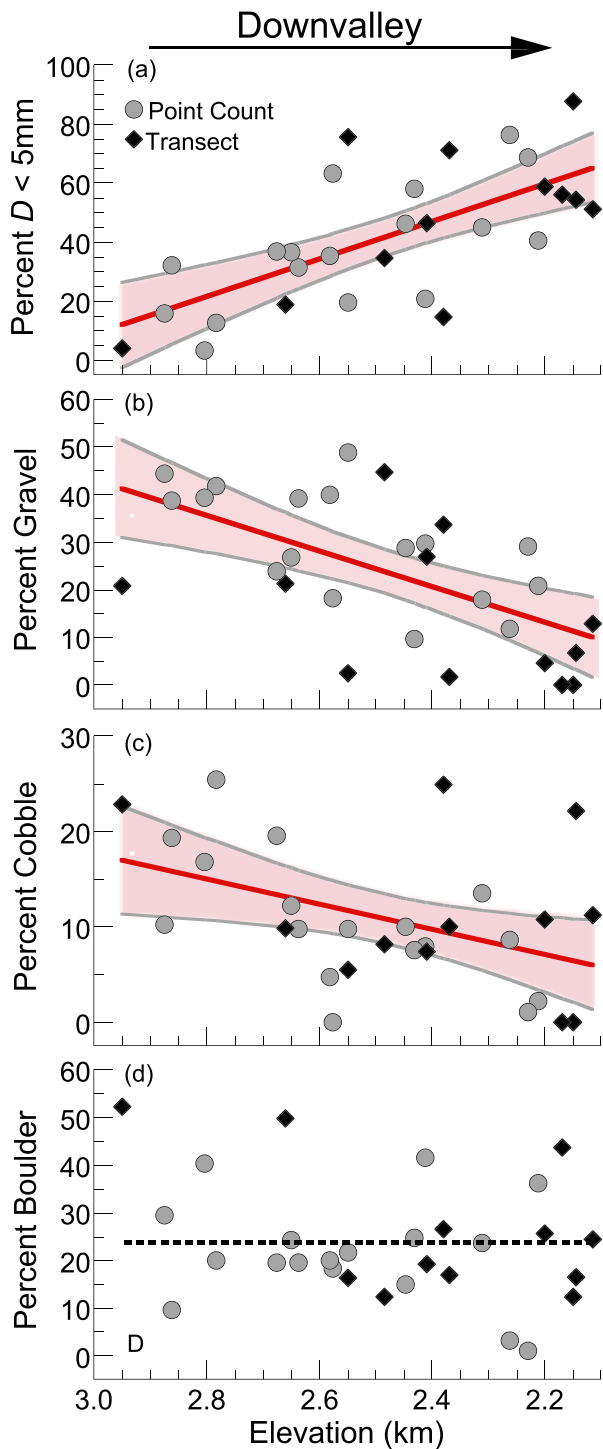


Figure 4. Comparison of transect and point count results. Variation with elevation of percentage of ground covered by sediment in four size-class bins: (a) $D < 5\text{ mm}$; (b) $5\text{ mm} < D < 64\text{ mm}$ (gravel); (c) $64\text{ mm} < D < 256\text{ mm}$ (cobble); and (d) $D > 256\text{ mm}$ (boulder). Downvalley fining trends from transect and point count measurements agree within error. Regression lines shown here were fit to combined data from these techniques ($n = 29$). See Figure 3 caption for explanation of regression lines and Table 1 for regression statistics. [Colour figure can be viewed at wileyonlinelibrary.com]

This suggests that the coarse mode represents blocks of rock that have been detached along preexisting bedrock fractures and are preserved on hillslopes without much reduction in size. Conversely, the variations in the fine mode are not reflected in the bedrock fracture spacing and therefore must be driven by some other factor or process that does vary with elevation.

Scree

One possible explanation for the observed downvalley fining in the fine mode is spatial variations in the production of scree, which we identified and measured as a distinct land cover type. As shown in Figure 8(a), the scree at the highest elevations is composed of coarse gravel and has a unimodal particle size distribution; scree particle sizes rarely exceed 128 mm, and thus do not overlap meaningfully with the coarse mode of the point count data (Figure 7). Scree becomes finer with decreasing elevation (and thus increasing distance downvalley), as revealed by statistically significant exponential trends in D_{16} , D_{50} , and D_{84} (Figure 8b–d). Moreover, scree and the fine mode of the point counts are correlated. The median size of scree matches the mean of the fine mode at high elevations, and both decline exponentially with decreasing elevation (Figure 8c). At the lowest elevations, the median is higher in the scree, compared to the fine mode of the point counts (Figure 8c). However, this may reflect a sampling bias rather than an altitudinal difference; the photographs of the scree only sample the surface, whereas the bulk samples taken for the point counts include material from the top 10 cm, implying that winnowing of fine material from the scree might explain some of the difference. The spread, quantified here as the geometric standard deviation, $\square_{\text{gsd}} = \log_{10}(D_{84}/D_{16})/2$, also decreases with decreasing elevation for both the scree and the fine mode of the point count distributions (Figure 8e). The slopes of the trends in the standard deviations of the scree and fine mode are not statistically distinguishable ($p = 0.70$), but the trends are offset – i.e. the average spread in scree is significantly lower than the average spread in the fine mode ($p < 0.0001$). The significantly narrower scree distributions support the hypothesis that scree represents a distinct population of hillslope sediment. Overall, the similarities in trends between the fine mode and the scree (Figure 8), suggest that the downvalley variations in particle size (Figures 6 and 8) are driven by altitudinal variations in weathering processes and are not tied to the more spatially uniform fracture spacing (Figure 7).

Implications for sediment production on hillslopes

Our field-based measurements of hillslope sediment in the Inyo Creek catchment show that higher elevation slopes produce coarser sediment, on average, consistent with previously published interpretations of cosmogenic nuclide and thermochronologic data from sediment sampled at the outlet (Riebe et al., 2015). Our new data also reveal the new finding that the sizes of sediment produced on hillslopes decline downvalley in a continuous exponential trend across the sampled elevation range (Figures 3, 4, and 8). Moreover, altitudinal trends in the relative abundance of different sizes are evident in all but the largest sizes, not just in the two size classes evaluated in previous work at the site (Stock et al., 2006; Riebe et al., 2015).

Results presented here also show that fracture spacing, in combination with elevation, helps explain the observed bimodal patterns in particle size distribution, consistent with a previously published theoretical framework for predicting size distributions of sediment produced on hillslopes (Sklar et al., 2017). In that framework, the initial size distribution depends on the latent size distribution (set by the spacing of weaknesses in bedrock), and is subsequently modified by weathering on hillslopes. Here, we see evidence for production of the catchment's coarsest sediment from fracture-bound

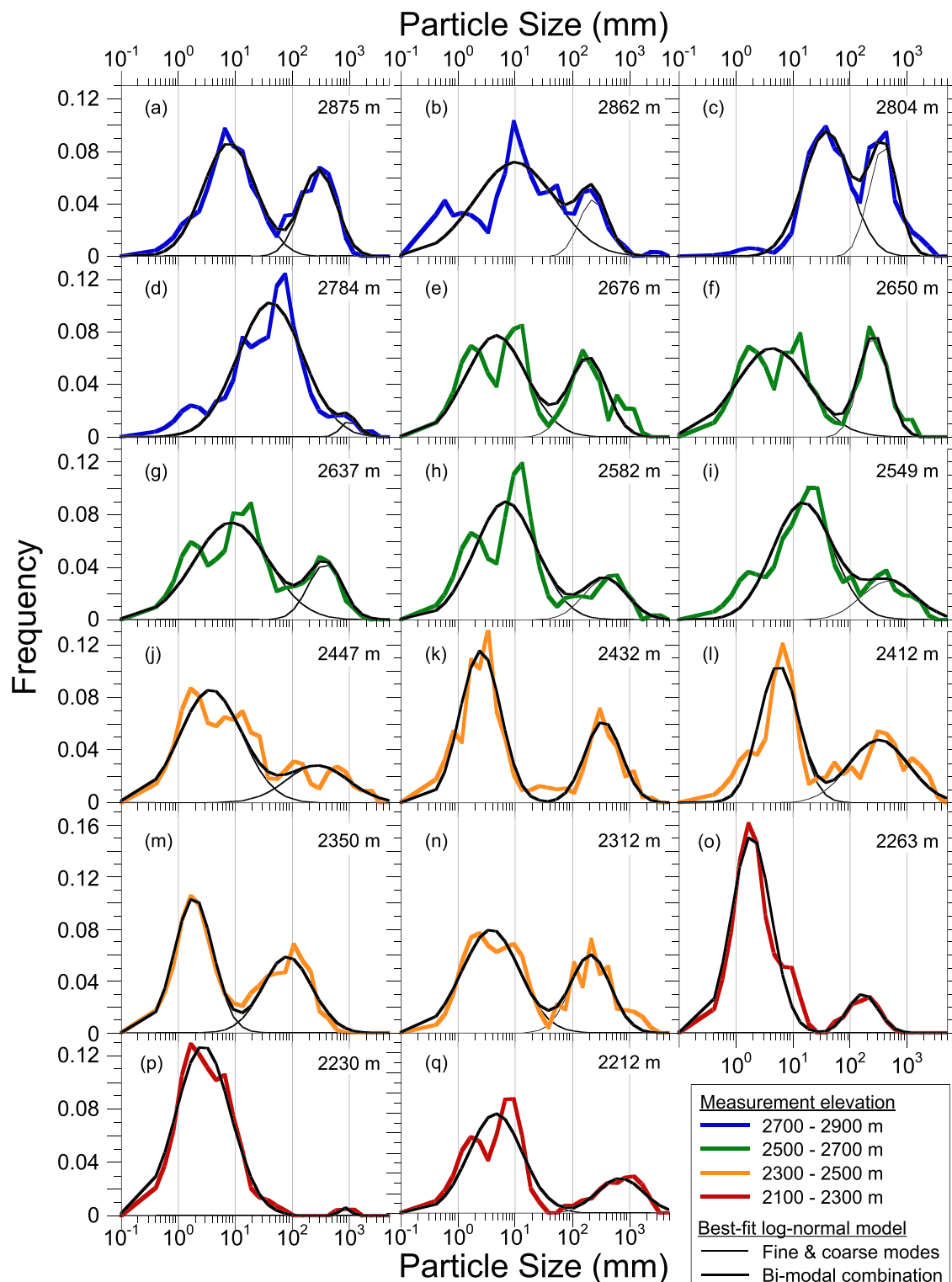


Figure 5. Bimodal distributions of surface particle size. Particle size distributions measured by point counting technique were fit with a bimodal log-normal probability density function; fine and coarse mode indicated by thin line, combined distribution by thick line. Best-fit parameters were estimated by non-linear optimization of five model parameters: the mean and standard-deviation of each mode, and a partitioning coefficient. Sample locations are displayed in order of descending elevation (a–q); colors distinguish elevations of sampling sites in 200 m intervals. Distributions are normalized so that area under curve = 1.0 for bin width = $\log_2(D) = 0.5$. [Colour figure can be viewed at wileyonlinelibrary.com]

blocks of unweathered bedrock (Figure 7). We also see downvalley fining that corresponds to altitudinal gradients in factors that influence the relative importance of chemical, physical, and biological weathering processes. Thus, our results provide empirical support for both of the main factors of the theoretical framework.

Our observation that 75% of the sediment produced on hillslopes occurs in the fine mode on average (Figure 6e), indicates that weathering dominates over the latent size distribution in the unweathered bedrock as a control on the measured particle size distributions in the Inyo Creek catchment. At other sites, in contrast, fracture spacing has been

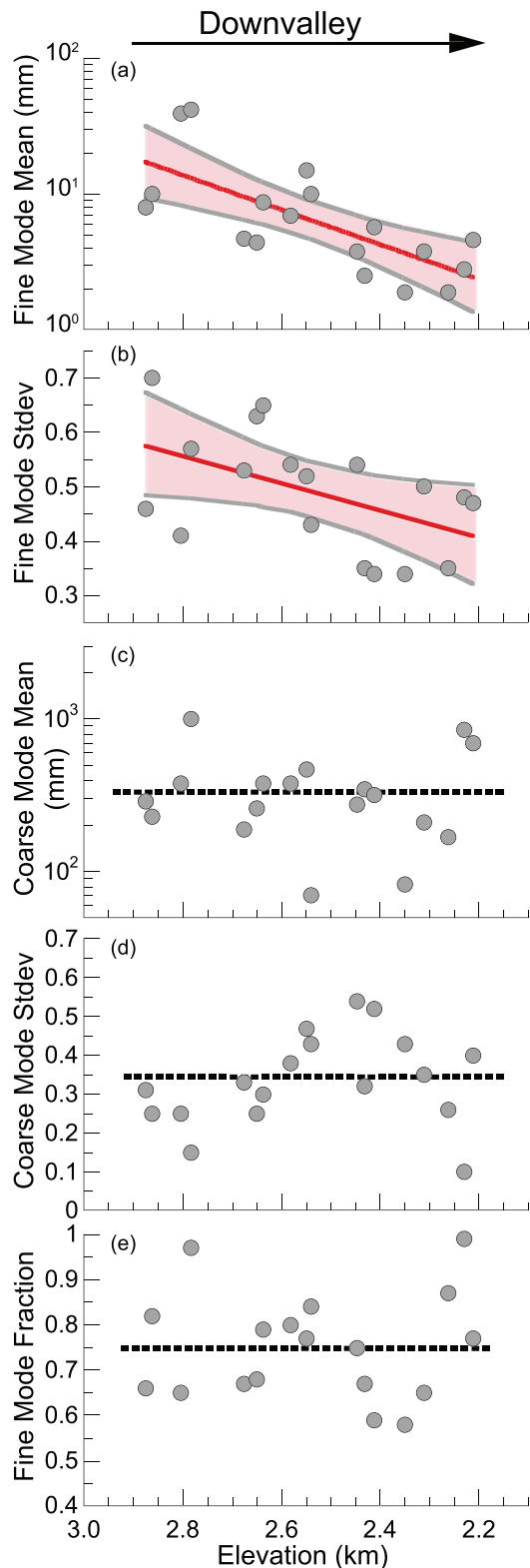


Figure 6. Downvalley trends in parameters of the bimodal model of log-normal particle size distributions. Significant downvalley fining is shown by the exponential decline in the fine-mode mean with decreasing elevation (a); spread in fine mode also narrows significantly downvalley (b). Coarse mode mean (c) and standard deviation (d), as well as fine-mode fraction (e), do not vary significantly with elevation. Note that the mean and standard deviation are calculated from the log-transformed values of particle size, i.e. $\log_{10}(D)$; for comparison with Figure 3, the values of the mean are displayed as untransformed particle size (in millimeters). See Figure 3 caption for explanation of regression lines and Table 1 for regression statistics. [Colour figure can be viewed at wileyonlinelibrary.com]

shown to play a key role in controlling sediment size distributions and erosion rates (DiBiase et al., 2018; Neely et al., 2019). Such site-to-site contrasts highlight the need for further study of factors that influence the relative importance of latent size distributions and weathering processes in setting grain size distributions of hillslope sediment supply.

The high relative abundance of the fine mode (Figure 6e), together with the wide gap between the coarse and fine modes at low elevations (Figure 5), suggests that the initial size distribution of sediment produced from bedrock can be controlled by weathering processes with little influence from the latent size distribution. We suggest that the processes that make the scree and drive the observed downvalley fining in the fine mode may reflect changes in the characteristic sizes of sediment produced by different processes. Coarser sizes found at higher elevations are produced by dominantly physical processes (e.g. frost cracking), while finer particles found at lower elevations are produced by dominantly chemical processes (e.g. disaggregation due to biotite weathering). At Inyo Creek, the altitudinal contrasts in physical, chemical, and biological processes are due to contrasts in hillslope gradient, ambient temperature, and forest cover (Riebe et al., 2015), which are common where relief is substantial. This implies that strong downvalley trends in hillslope sediment size are likely present in other mountain landscapes around the world.

Implications for downstream fining

Our field measurements of hillslope sediment size support the hypothesis, proposed in previous work (e.g. Sklar et al., 2006), that downstream fining in mountain rivers can be driven in part by downvalley variations in weathering processes on hillslopes. Over the 10^3 - to 10^4 -year timescales of sediment production (Sklar et al., 2017), downvalley fining of sediment produced on hillslopes should lead to a downstream decrease in the supply of relatively coarse particles and a downstream increase in the supply of relatively fine particles to the channel network. This in turn leads to a downstream shift in the particle size distribution of the overall mass flux in the channel toward a greater proportion of suspitable sizes (e.g. sand and finer) and a lesser proportion of non-suspitable coarser material, even as the overall flux increases due to cumulative additions of sediment from adjacent slopes. It should also lead to downstream fining in the particle size distribution of the flux of non-suspitable material (e.g. gravel and coarser). Any downstream fining of the long-term average bedload flux may in turn drive downstream variations in the size distribution on the river bed surface, which for any reach of river is ultimately created by vertical and lateral sorting of particles supplied from upstream. However, the size distribution of the long-term average sediment flux passing any point in the channel network is also affected by particle abrasion during transport downstream. This raises two questions: How does the combination of downvalley fining of hillslope sediment and particle abrasion during transport influence downstream fining in the size distribution of the long-term average sediment flux carried by mountain rivers? And what are the resulting downstream variations in both the proportion and the size distribution of the non-suspitable (coarse) component of the sediment flux.

To answer these questions, we applied a forward model of hillslope sediment production and downstream transport to the DEM of the Inyo Creek catchment (Lukens et al., 2016; Sklar et al., 2016). The goal was to predict downstream variations in the size distribution of the long-term average sediment flux from the measured altitudinal variation in hillslope sediment size, for a wide range of abrasion rates. These predictions

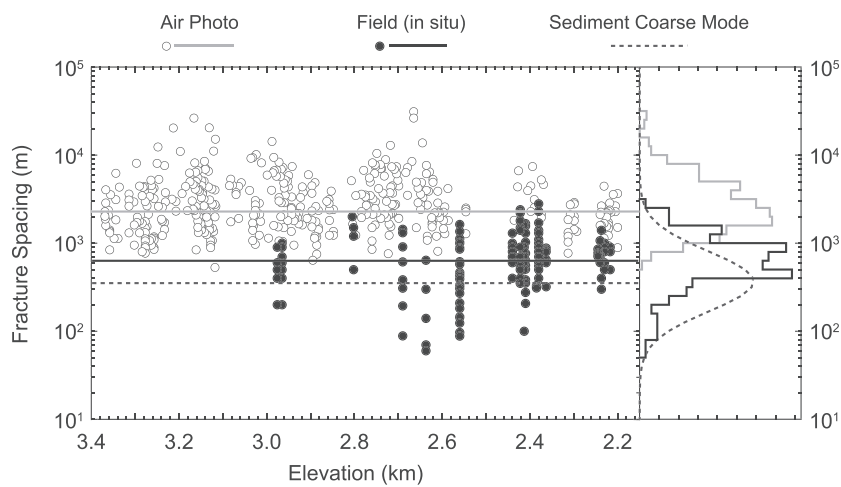


Figure 7. Bedrock fracture spacing. Variations in spacing between fractures in exposed bedrock, measured directly in the field (filled circles) and remotely from orthorectified aerial photographs (open circles). Fracture spacing is not strongly correlated with elevation in either field (black) or aerial photograph (gray) data. Horizontal lines show median values for distributions measured in the field and from aerial photographs. Dashed line shows mean of the coarse-mode of the bimodal model fit to point-count measurements. Histograms at right show fracture spacing distributions (gray and black lines) and distribution of the modeled coarse mode (dashed line).

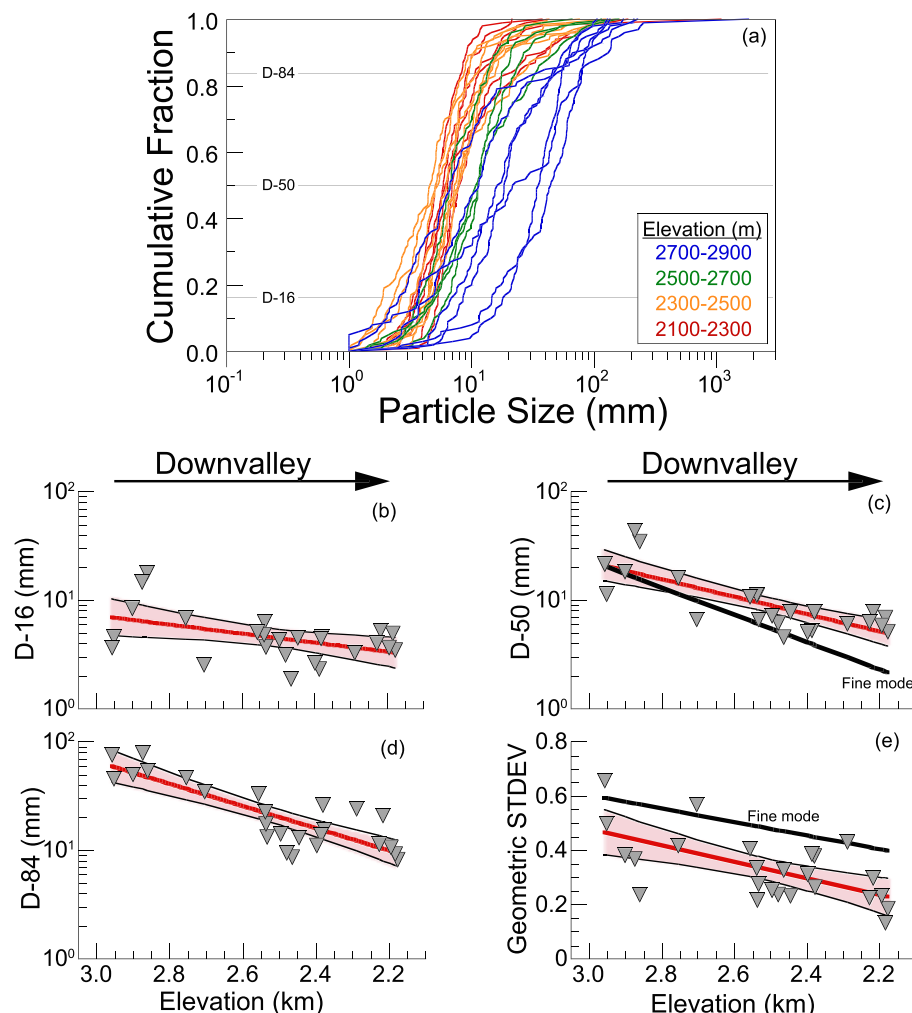


Figure 8. Grain size distributions from scree slopes. (a) Cumulative particle size distributions for 25 scree slope locations measured by photo-sieving (see text). Colors vary from cool for high elevations to warm for low elevations. (b–e) Results show significant downvalley fining of 16th, 50th, and 84th percentiles, and narrowing of geometric standard deviation with decreasing elevation. See Figure 3 caption for explanation of regression lines and Table 1 for regression statistics. Black lines in (c) and (e) show trends in the mean and standard deviation of the fine mode derived from bimodal log-normal fits to point count data (Figure 6). [Colour figure can be viewed at wileyonlinelibrary.com]

are not readily validated, because we do not know either the abrasion resistance or the particle size distribution of the bedload flux at Inyo Creek. Nevertheless, because the model is parameterized with a measured pattern of downvalley fining, the output should provide insight into the relative importance of downvalley fining and abrasion in steep mountain catchments.

The model tracks the inputs and outputs of mass for each size class in the sediment flux as a function of travel distance to the outlet. We outline our approach in the paragraphs that follow and provide a detailed description of the model equations and calculations in the Supporting Information, Data S2, available with the online version of this article. Here we highlight two key simplifying assumptions. First, we assumed that, over a timescale long enough to encompass transport events that move the largest particles, all sediment mass produced on hillslopes is transported down slopes and through the channel network. This implies that local slope and channel geometry are adjusted to transport the full size distribution of sediment supplied from upstream, with full connectivity (Wohl et al., 2019) along sediment transport pathways. As a result, there is no long-term net deposition of any sediment particle size class within the channel network. The second key assumption is that the rate of particle size reduction by abrasion is spatially uniform, irrespective of whether particles are moving down hillslopes or along channels. This implies that the net effect of physical and chemical weathering is equally efficient at particle size reduction along each segment of the transport pathway from hillslope source to catchment outlet.

Forward model of downstream fining of sediment flux

In the model, at each point (pixel) on the landscape, sediment produced by erosion of bedrock has a particle size distribution determined by parameters quantified in our regression analysis of the fine and coarse modes of the measured distributions (Figure 6). Thus we assumed that the measured altitudinal trends in the fine mode (Figure 6a, b) and the spatially uniform coarse mode (Figure 6c, d) are representative of trends on hillslopes throughout the catchment, including elevations above 2900 m, which we were unable to sample. In addition, we assumed that the fine and coarse modes of the hillslope sediment size distributions can be combined according to a 3:1 ratio at every point on the landscape (Figure 6e).

Figure 9 shows how the modeled hillslope particle size distributions vary with elevation. At the highest elevations, the fine and coarse modes overlap, producing a unimodal distribution that peaks at ~300 mm and includes 10 m boulders, consistent with the largest particles we observed in the field (Figure 2i). As elevation decreases downvalley, the fine mode separates from the coarse mode, yielding a wide and weakly bimodal distribution (Figure 9a), consistent with our observations at middle elevations (Figure 2c). At the lowest elevations, near the catchment outlet, little sediment is produced in the 10–100 mm size range (Figure 9a), leaving only boulders and gruss (Figure 2d). Overall, median particle size decreases exponentially with elevation, while the fraction > 2 mm is close to 1, except at the lowest elevations (Figure 9c), consistent with previous findings that sand and fine gravel are preferentially sourced from low elevations in this catchment (Riebe et al., 2015).

Elevation can also influence the rate that sediment is produced at each point on the landscape, due to the effects of altitudinal variations in climate and topography on erosion

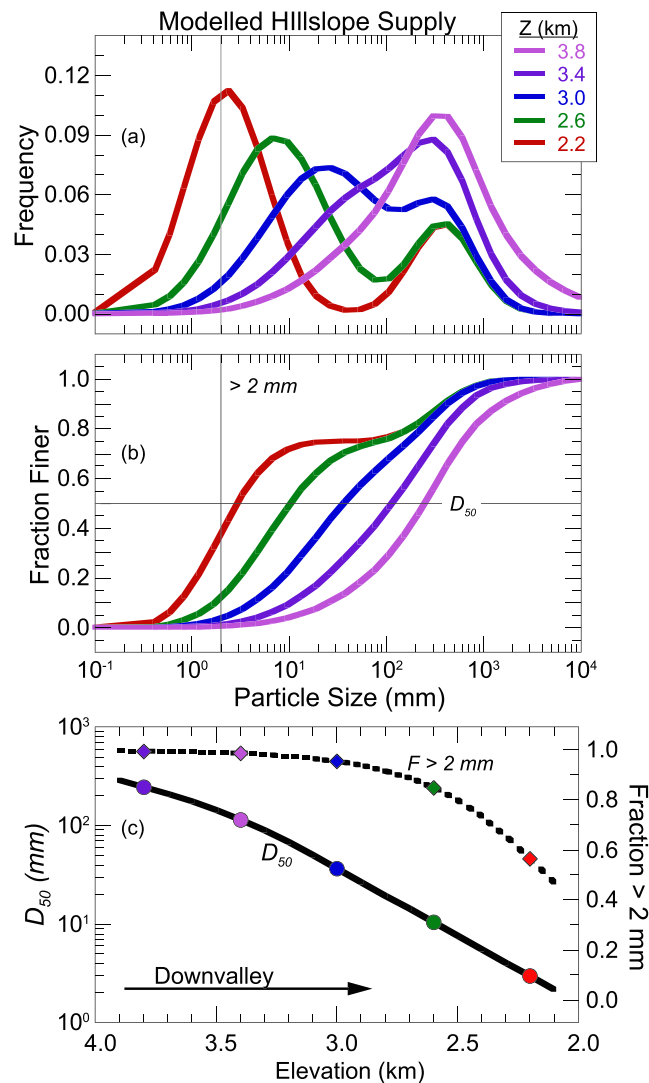


Figure 9. Modeled catchment-wide particle size distributions. Variations with elevation of bimodal distributions fit to point count data, shown as probability density functions (a) and cumulative distributions (b) for representative elevations from the range spanned by Inyo Creek. (c) Median particle size (solid line) and fraction (F) greater than 2 mm (dashed line) as continuous functions of elevation show predicted downvalley fining of sediment produced on hillslopes, assuming that regression parameters from bimodal fits to point count data are representative of sediment size distributions throughout Inyo Creek catchment. [Colour figure can be viewed at wileyonlinelibrary.com]

rates. Locations with higher erosion rates (e.g. due to steeper slopes) contribute more sediment to the channel per unit area and thus have a greater influence on the size distribution of channel bed sediment. We considered two scenarios in our modeling exercises: One in which erosion rates are spatially uniform and one in which erosion rates increase as a power function of elevation, consistent with cosmogenic nuclide data from Inyo Creek (Riebe et al., 2015).

In addition to having a particle size distribution and erosion rate, each pixel in the catchment has a travel distance to the outlet (Figure 1b), which can be calculated from the DEM. The travel distance influences the amount of particle size reduction during transport to the outlet. Here we model particle size reduction as a simple exponential function of travel distance, which is expressed in differential form in Equation 1

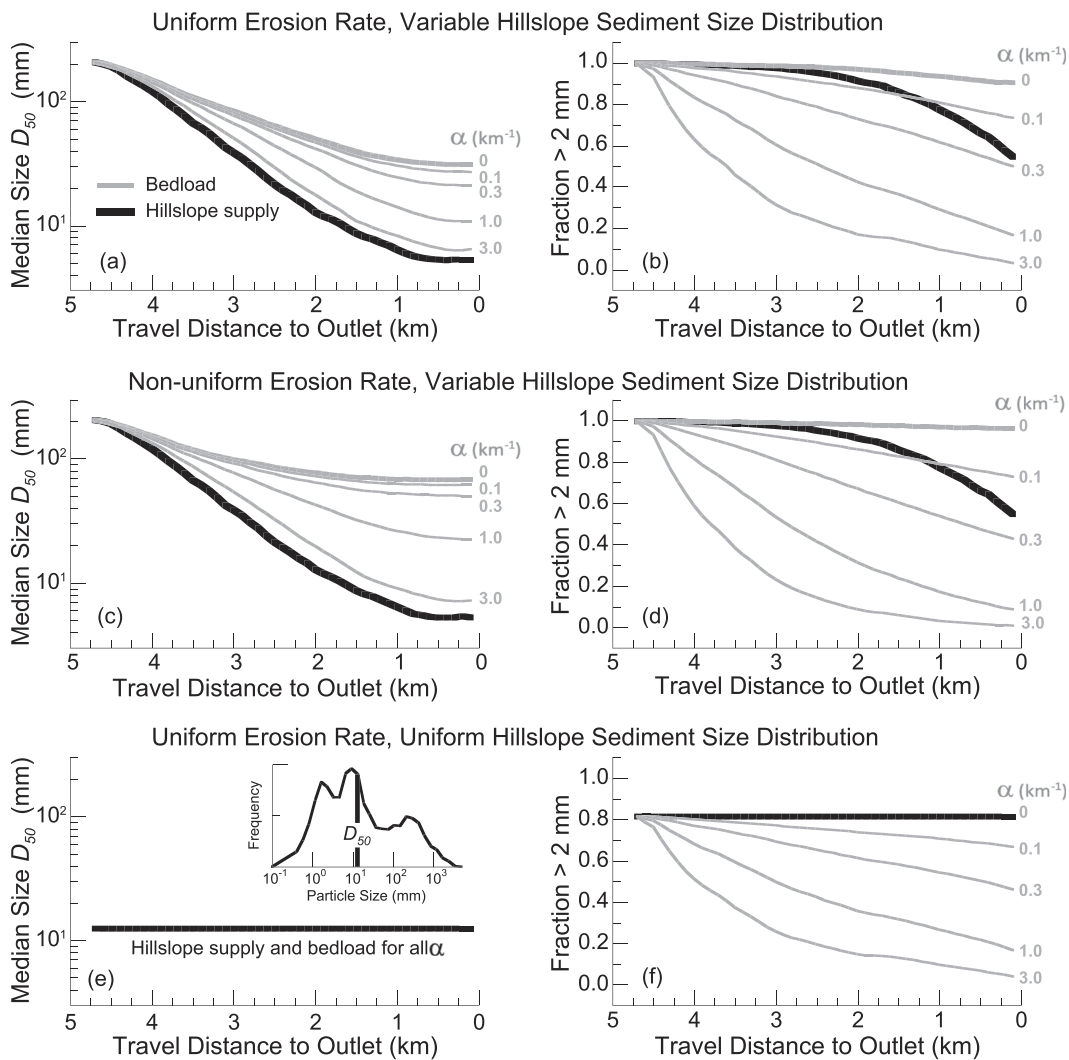


Figure 10. Modeled downstream fining of long-term average bedload flux due to combined effects of downvalley fining of hillslope sediment size and particle abrasion in transport. The model simulates the downstream evolution of the size distribution of the sediment flux by solving the mass balance for each particle size class. It accounts for mixing of sediment from source areas with differing erosion rates and production of sand and silt by abrasion of coarse particles. We assume that over a sufficiently long timescale, all sediment is transported through the catchment, i.e. there is no net long-term sediment deposition of any size class. Panels (a), (c) and (e) show downstream variations in the median particle size (D_{50}) of the hillslope supply (black lines) and the average bedload flux (i.e. $D > 2$ m, gray lines), for a range of abrasion coefficients. Panels (b), (d), and (f) show the downstream variations in the fraction of the hillslope sediment supply (black lines) and total sediment flux (gray lines) composed of particles with $D > 2$ mm. Results include scenarios where erosion is either spatially uniform or varies as a power function of elevation (after Riebe et al., 2015). Size distributions of sediment produced on hillslopes vary with elevation as shown in Figure 9 for (a–d), or are spatially uniform for (e–f), with size distribution shown in the inset of panel (e). Model results show that downvalley fining of hillslope sediment is necessary for downstream fining of the average bedload flux. Abrasion plays a secondary role in controlling bedload D_{50} by modulating the fining rate imposed by hillslope supply. For sediment with high abrasion coefficients (i.e. weak rock), bedload flux will mirror the size distribution of sediment produced on adjacent hillslopes. In all cases, abrasion plays a dominant role in controlling the partitioning of sediment flux between bedload and suspended load.

$$dM/dL = -\alpha M \quad (1)$$

where dM/dL is the rate of change in particle mass (M) per unit travel distance (L), and α is the spatially uniform susceptibility of sediment to abrasion. We assume that mass lost from abrading particles is converted to sand and silt-sized particles, which travel in suspension during floods. We only calculate mass loss to abrasion for gravel and larger-sized particles, assuming that the boundary between sand and gravel, i.e. $D = 2$ mm, is a characteristic size for partitioning long-term flux between suspended load and bedload, and that particles traveling in suspension are not abraded before reaching the gravel-sand transition in bed material at lower gradient channels downstream of the mountain front (Dingle et al., 2017).

To quantify how the size distribution of the integrated sediment flux varies with distance downstream, we divide the catchment into 100 m travel distance bins and calculate the mass balance of sediment in each size class at each travel distance bin. The mass balance accounts for supply from upstream; local supply from hillslope sediment production; and changes in mass due to abrasion. Our model uses Equation 1 to track both the mass of the original particles and the mass of suspendable particles (sand and silt) that are produced as byproducts of abrasion. This results in two types of mass transfer during transport downstream: from one size class to the next smaller size class and from all coarse sizes to the sand and finer size class (i.e. the byproducts of abrasion). Thus our mass balance model tracks all inputs and outputs for all size classes at all travel distances to the outlet (model equations and their application to the Inyo Creek topographic and sediment size data are described in detail in the Supporting Information, Data S2).

Trade-offs between abrasion and hillslope sediment supply

We used the mass balance model to calculate variations in the D_{50} of the fraction of the total flux with $D > 2 \text{ mm}$ (i.e. gravel-sized and coarser sediment, which we refer to as the 'long-term average bedload flux.') As shown in Figure 10(a), the D_{50} of the fraction of hillslope sediment supply with $D > 2 \text{ mm}$ is greatest for source locations far from the outlet, declining from 200 mm at those locations to roughly 5 mm at source locations closest to the outlet, reflecting the altitudinal trends in particle size distribution (Figure 9) and the close correlation between elevation and travel distance to the outlet (Figure 1b). The downstream fining of the bedload flux is more gradual in the absence of abrasion (i.e. $\alpha = 0 \text{ km}^{-1}$), from 200 mm to roughly 30 mm in the case of spatially uniform erosion (Figure 10a). This is due to the downstream accumulation of sediment mass, which dilutes inputs of finer sediment produced at travel distances closer to the outlet. As the susceptibility to abrasion increases over the range from $\alpha = 0.1 \text{ km}^{-1}$ to 3.0 km^{-1} , the rate of downstream fining increases (Figure 10a), because mass from upstream sources is increasingly transferred to sand and finer sizes that do not contribute to the bedload flux (Figure 10b). However, the downstream fining rate is limited by the rate of downvalley fining of hillslope sediment; for $\alpha > 3.0 \text{ km}^{-1}$, the D_{50} of the bedload flux matches the D_{50} of the hillslope sediment supply. In this limiting case, which corresponds to extremely weak bedrock, virtually all sediment is rapidly converted to particles with $D < 2 \text{ mm}$, such that the long-term average coarse sediment flux at any travel distance is derived solely from local sources (Figure 10b).

The general pattern of tradeoffs between abrasion and hillslope sediment supply is also evident when erosion rates increase as a power function of elevation (Figure 10c, d). However, downstream fining of the median size of the long-term average bedload flux is less pronounced, declining from 200 mm to just 68 mm for $\alpha = 0.0 \text{ km}^{-1}$ (no abrasion), because locations that produce finer sediment (i.e. closer to the outlet) erode more slowly and contribute less sediment to the bedload flux (Figure 10c). As the susceptibility to abrasion increases, the altitudinal increase in erosion rates is overwhelmed by the weakness of the bedrock, and the downstream fining in bedload converges with downvalley fining of hillslope sediment supply when $\alpha > 3.0 \text{ km}^{-1}$, similar to the uniform erosion case (cf. Figure 10a, c). Compared to the case of uniform erosion, abrasion in the non-uniform erosion case has more influence on the partitioning of the long-term average flux between the fine and coarse fractions, because more of the sediment is produced at longer travel distances to the outlet and is therefore more affected by abrasion (cf. Figure 10b, d).

Our model suggests that downvalley fining in sediment supply is the dominant control on downstream fining of the long-term average coarse sediment flux and that abrasion plays a secondary role, modulating the relative importance of upstream and local sediment sources. Moreover, downvalley fining may be necessary for downstream fining of the long-term flux, as indicated by model results for cases in which hillslopes produce sediment with a spatially uniform particle size distribution (Figure 10e). In these scenarios with no downvalley fining, we set the size distribution of sediment produced by erosion on hillslopes (Figure 10e, inset) to be equal to the average of all particle size distributions measured using the point counting technique at Inyo Creek (Figure 3a). As shown in Figure 10(e), the D_{50} of the bedload always equals the D_{50} of the hillslope sediment supply (i.e. 12 mm), irrespective of the abrasion coefficient.

Though this result may initially seem counterintuitive, it can be understood by considering the end member cases of very weak and very strong bedrock (i.e. high and low α). When abrasion is negligible ($\alpha = 0 \text{ km}^{-1}$), there is no mechanism for changing the size distribution of the long-term average sediment flux; it equals the hillslope sediment size distribution, which does not vary downvalley. When abrasion is very efficient ($\alpha > 3.0 \text{ km}^{-1}$), the bedload flux mirrors the hillslope inputs for the same reason that it does so in the case of downvalley fining (Figure 10a, c); virtually all sediment is rapidly converted to suspendable particles with $D < 2 \text{ mm}$ (Figure 10f), and the coarser sediment flux at any travel distance is derived solely from local sources. When rock strength is intermediate (i.e. for intermediate α), particles are reduced in size more gradually, but most of the mass is converted to sizes that are carried away in suspension. For example, only 12% of the mass is retained in the bedload flux when the diameter of a nominally spherical particle is reduced by a half. In addition, for any size class, the mass transferred to the next smaller size class in each travel distance bin is at least partly compensated by mass added from abrasion of particles in the next larger size class. Moreover, the continuous additions of hillslope-derived material with a spatially uniform size distribution overwhelms any shifts caused by imbalances in the transfers between particle size classes. This result confirms previous work (Sklar et al., 2006), which demonstrated analytically that when hillslope sediment size does not vary spatially, extremely narrow size distributions are required for abrasion to result in measurable downstream fining of the long-term average bedload sediment flux.

Together, our modeling exercises point to three key findings about downstream fining of sediment flux in mountain landscapes, assuming hillslopes and channels are closely coupled and net sediment deposition can be neglected because all particle sizes are mobile over sufficiently long timescales. Firstly, downvalley fining of hillslope sediment supply is necessary to produce downstream fining in the long-term average flux of coarse, non-suspendable sediment, irrespective of rock resistance to abrasion. This is contrary to the prevailing view – i.e. that abrasion is solely responsible for downstream fining in the absence of long-term net deposition of the coarse tail of the bedload sediment size distribution (e.g. Kodama, 1994; Miller et al., 2014), to the extent that river bed size distributions are affected by sediment supply from upstream. Secondly, the effect of abrasion on the size distribution of the non-suspendable flux is limited to modulating the more dominant effect of downvalley fining of hillslope sediment supply. As the rate of abrasion increases, the size distribution of the long-term average bedload flux more closely mirrors the size distribution of local sources of hillslope sediment. The correspondence is especially strong when the hillslope sediment size distribution is wide, as may often be the case based on data from mountain landscapes around the world (Casagli et al., 2003; Attal et al., 2015; Haddadchi et al., 2018; Roda-Boluda et al., 2018). Thirdly, abrasion and hillslope sediment size interact to control the partitioning of the long-term average sediment flux between the bedload and suspended load. In catchments such as Inyo Creek, where hillslopes produce sediment with sizes that are mostly greater than sand, abrasion creates much of the suspended load and limits downstream increases in bedload flux, even as contributing area increases. These findings, which are based on field data from Inyo Creek, confirm earlier modeling (Sklar et al., 2006) of the effects of abrasion and hillslope sediment supply on long-term average sediment flux. They should apply anywhere hillslope sediment size varies across the landscape (Sklar et al., 2017) and anywhere abrasion is effective at converting the coarse load to sand and silt (e.g. Dingle et al., 2017).

Links between the long-term average bedload flux and riverbed sediment size

One question our modeling does not answer that needs to be addressed in future work is: How does the modeled downstream fining of long-term average bedload flux affect downstream fining of riverbed surface size distributions? We hypothesize that downstream fining in the bedload flux can affect size distributions of bed surface sediment for three reasons. First, the bed surface is constructed from the range of particle sizes supplied by the long-term average bedload flux. Second, spatial and temporal variations in the bed surface sediment size distribution can generally be interpreted as systematic deviations around the baseline particle size distribution supplied by the long-term average bedload flux. Third, these systematic deviations are influenced by the magnitude of the bedload flux, which covaries with the downstream fining of long-term average bedload flux according to our model (cf. right and left panels in Figure 10). Testing this hypothesis will require scaling up in time and space what is currently known about mechanisms that underlie variability in surface size distributions.

One source of variability is temporal fluctuations in the supply of water and sediment from slopes and tributaries. Measurements of riverbed size distributions, which provide the basis of published observations of downstream fining (e.g. Kodama, 1994; Miller et al., 2014), generally provide only a snapshot of the state of the river at a moment in time. As a result, they may reflect transient responses to recent events, such as floods (Thompson and Croke, 2013) and debris flows (Wohl and Pearthree, 1991), or pulses of elevated sediment supply from landslides (Cui and Parker, 2005) or mine waste (Ferguson et al., 2015). This could lead to relatively short-lived ($\sim 10^0\text{--}10^2$ year) fluctuations in riverbed size around its long-term average.

In addition to temporal fluctuations, there are persistent deviations due to vertical sorting that make the riverbed surface systematically coarser than the subsurface size distribution, which is more characteristic of long-term average bedload (Parker and Klingeman, 1982). In gravel bed rivers, the median size of the resulting coarse surface layer is commonly a factor of two to six greater than the median of the subsurface size distribution (Hassan et al., 2006; Pitlick et al., 2008). If the size distribution of the long-term average bedload flux decreases downstream, then the size distribution of the coarse surface layer should also decrease downstream, because the coarsening is a deviation from a systematically finer baseline source of sediment. The downstream fining of the bedload flux may also influence the degree of surface coarsening because it results in a downstream reduction in the fraction of coarse (> 2 mm) sediment in the long-term average total flux (Figure 10 b–d, f). A reduced coarse sediment supply, combined with a downstream increase in drainage area and thus discharge, could in turn lead to a larger ratio of surface to subsurface sediment size (Dietrich et al., 1989; Buffington and Montgomery, 1999a; Hassan et al., 2006).

In addition to affecting vertical sorting, downstream changes in the fraction of coarse sediment in the long-term average flux can also drive spatial variations in bed surface size distribution due to lateral sorting at the scale of individual reaches. Lateral sorting, which has been shown to vary inversely with coarse sediment flux (Nelson et al., 2009), subdivides the size distribution of the long-term average flux into spatially distinct patches of relatively uniform sizes (Buffington and Montgomery, 1999b). This complicates characterization of downstream fining in riverbeds. For example, if measurements are limited to point bars, as is often the case in downstream fining observations (e.g. Attal and Lavé, 2006), the measured particle size distributions

could be systematically offset from and thus vary downstream in parallel to the long-term average bedload size distribution. Alternatively, the downstream trends may diverge if point bars become less representative of the spatially averaged bed surface.

Vertical and lateral sorting arise because larger, more massive particles are less mobile for a given shear stress (Ashworth and Ferguson, 1989; Mao et al., 2008), and shear stress varies both in time and space across the channel (Ferguson, 2003). The resulting size-selective transport can produce downstream fining in riverbed sediment in depositional settings (Paola et al., 1992; Ferguson et al., 1996; Gomez et al., 2001), where accommodation space allows for long-term storage of the less mobile, coarse tail of the long-term average bedload flux. However, size selective transport over short timescales does not preclude full mobility of all sizes over long timescales for channels with no net deposition – i.e. channels that have the range of shear stresses over time that can collectively transport all sizes in proportion to their long-term average supply from upstream. At the timescale of individual transport events, gravel riverbeds are systematically coarser than the measured bedload flux, particularly when shear stress is only slightly higher than the critical stress required to initiate bedload transport (Mao et al., 2008). At higher shear stresses, the bedload size distribution is typically coarser and becomes approximately equal to the surface size distribution at the highest magnitude and lowest frequency discharges (Ashworth and Ferguson, 1989; Ferguson et al., 1996; Lenzi et al., 1999; Mao and Lenzi, 2007). Thus, when integrated over the full range of discharges, all sizes present on the bed, including the coarsest particles, can be moved downstream at their long-term rate of supply from upstream (Parker and Toros Escobar, 2002), leading to no net deposition, as assumed in our model.

The assumption of no net long-term deposition should be valid in many mountain settings characterized by active rock uplift and river incision into bedrock. Exceptions occur where accommodation space is created locally by downdropping of blocks along normal faults, damming of valleys by landslides or glaciers, and valley widening and floodplain development that creates surfaces adjacent to the channel where fans are deposited. Another exception to our model assumptions can occur in antecedent rivers entrenched in isolated gorges, where little additional sediment is supplied by hillslopes and elevation change is small compared to local relief. However, even in these exceptional cases, understanding downstream fining of the bed requires consideration of the long-term average bedload flux from which the riverbed is built.

Our mass-balance model was not designed to quantify how downstream fining of the long-term average bedload flux influences downstream fining of river bed size distributions. However, several recently published river longitudinal profile models include many of the components needed: relationships for mixed-particle-size bedload transport and vertical sorting; particle size reduction by abrasion; and the potential to include temporal variations in discharge and spatial variations in the sediment size distribution supplied to the channel (e.g. Cui and Parker, 2005; Ferguson and Church, 2009; Chatanantavet et al., 2010; Ferguson et al., 2015). Yet applications of these models have held input sediment size distributions constant and parameterized hydrologic variability with a single, intermittent, effective discharge. Our findings at Inyo Creek, showing strong downvalley fining of hillslope sediment size and downstream fining of long-term average sediment flux, highlight the need to include these effects in future modeling of bed surface sediment size along river longitudinal profiles.

Conclusions

Sediment size plays a fundamental role in a wide range of Earth surface processes, yet we lack a comprehensive understanding of how particle size distributions evolve from source to sink. In particular, relatively little work has been done to quantify sediment size distributions at their points of origin on hillslopes, and even less has been done to understand the factors that cause them to vary across mountain landscapes. Our field study represents the first catchment-scale analysis of spatial variations in the size distributions of sediment produced on hillslopes. We found an exponential downvalley decrease in all but the largest sampled particle sizes across the range of sampled hillslopes. Measured size distributions are bimodal, with a coarse, bouldery mode that is spatially uniform and a more abundant fine mode that shifts downvalley from cobbles to gravel and finally to sand near the catchment outlet. The sizes in the coarse mode are similar to measured bedrock fracture spacings, which are also spatially uniform. The downvalley shift in the fine mode is consistent with changes in the relative importance of physical, chemical, and biological weathering as a function of elevation.

We used the observed patterns of downvalley fining in a forward model that reveals the relative importance of downvalley fining and particle abrasion in downstream fining of the long-term average bedload sediment flux. Model outputs show that downvalley fining of hillslope sediment is a necessary condition for downstream fining of the bedload sediment flux in mountain landscapes where hillslopes and channels are strongly coupled, with implications for downstream fining in riverbed sediment. Abrasion plays a secondary role in downstream fining of the long-term average bedload flux, but plays a dominant role in partitioning it between bedload and suspended load. Our observations, though limited to Inyo Creek, result from processes that are likely widespread in mountain ranges around the world and therefore have broad implications for understanding the role of particle size in mediating feedbacks between climate, tectonics, and mountain landscape evolution.

Understanding how these feedbacks work at Inyo Creek will require a complete understanding of the evolution of sediment from its origins on slopes to its flux out of the catchment. Our findings thus far provide unprecedented insight into several stages of sediment evolution in a steep mountain catchment. This study, which is part of an ongoing program of research, showed that surface particle size distributions become finer with decreasing elevation and thus with increasing distance downvalley, a phenomenon we refer to as downvalley fining. In previous work, we used isotopic data to show that coarse gravel passing through the Inyo Creek outlet is preferentially sourced from higher elevations relative to finer sediments, which we interpret as a response to altitudinal gradients in physical, chemical, and biological weathering processes (Riebe et al., 2015). This interpretation is consistent with a recently developed theoretical framework for understanding how bedrock properties and weathering processes combine to influence the size distributions of hillslope sediment (Sklar et al., 2017). In addition, modeling of sediment size evolution confirms that downvalley fining can dominate over abrasion as a source of downstream fining of the long-term average bedload sediment flux (Sklar et al., 2006). However, at least four additional advances are needed to complete the picture of how sediment size evolves from source to sink at Inyo Creek:

- identify source elevations for all particle sizes delivered to the outlet by extending the analyses of cosmogenic nuclides

and detrital thermochronology to all particle sizes in the stream;

- link the hillslope sediment size measurements to the isotopic data from the outlet by accounting for particle size reduction by abrasion and fragmentation in transport by fluvial and debris flows;
- quantify how bed surface size distributions are influenced by downstream changes in the size distribution of the long-term bedload flux in steep mountain catchments such as Inyo Creek;
- develop, test, and refine predictive models of how altitudinal variations in chemical, physical, and biological processes influence the production and weathering of sediment on hillslopes.

Acknowledgements—Funded by the National Science Foundation (USA) grants EAR 1324830 to Sklar and EAR 1325033 to Riebe. Additional support for Sklar, Genetti, and Leclerc provided by the Doris and David Dawdy Fund for Hydrological Science at San Francisco State University. The authors thank Nick Aiello, Omid Arabnia, Gionata Bianchi, Theresa Fritz-Endres, Gabriella Geyer, E. Gilliam, Jason Guldman, Andrea Key, Mobin Mahmoudi, Molly McLaughlin, David Quicke, Sam Shaw, and Joey Verdian for assistance in the field. Review comments by Rob Ferguson and Mitch D'Arcy significantly improved this article.

Conflict of Interest

All authors have no conflicts of interest to declare.

Data Availability Statement

The data that supports the findings of this study are available in the Supporting Information of this article.

References

- Arabnia O, Sklar LS. 2016. Experimental study of particle size reduction in geophysical granular flows. *International Journal of Erosion Control Engineering* **9**(3): 122–129.
- Ashworth PJ, Ferguson RI. 1989. Size-selective entrainment of bed load in gravel bed streams. *Water Resources Research* **25**(4): 627–634.
- Attal M, Lavé J. 2006. Changes of bedload characteristics along the Marsyandi River (central Nepal): implications for understanding hill-slope sediment supply, sediment load evolution along fluvial networks, and denudation in active orogenic belts. *Tectonics, Climate, and Landscape Evolution* **39**: 143–171.
- Attal M, Mudd SM, Hurst MD, Weinman B, Yoo K, Naylor M. 2015. Impact of change in erosion rate and landscape steepness on hillslope and fluvial sediments grain size in the Feather River basin (Sierra Nevada, California). *Earth Surface Dynamics* **3**(1): 201–222.
- Blom A, Viparelli E, Chavarriás V. 2016. The graded alluvial river: profile concavity and downstream fining. *Geophysical Research Letters* **43**(12): 6285–6293.
- Booth DB, Leverich G, Downs PW, Dusterhoff S, Araya S. 2014. A method for spatially explicit representation of sub-watershed sediment yield, southern California, USA. *Environmental Management* **53**(5): 968–984.
- Brocklehurst SH, Whipple KX. 2004. Hypsometry of glaciated landscapes. *Earth Surface Processes and Landforms* **29**(7): 907–926.
- Buffington JM, Montgomery DR. 1999a. Effects of sediment supply on surface textures of gravel-bed rivers. *Water Resources Research* **35**(11): 3523–3530.
- Buffington JM, Montgomery DR. 1999b. A procedure for classifying textural facies in gravel-bed rivers. *Water Resources Research* **35**(6): 1903–1914.
- Callahan RP, Ferrier KL, Dixon J, Dosseto A, Hahm WJ, Jessup BS, Miller SN, Hunsaker CT, Johnson DW, Sklar LS, Riebe CS. 2019. Arrested development: Erosional equilibrium in the southern Sierra Nevada, California, maintained by feedbacks between channel

- incision and hillslope sediment production. *Geological Society of America Bulletin* **131**(7–8): 1179–1202.
- Casagli N, Ermini L, Rosati G. 2003. Determining grain size distribution of the material composing landslide dams in the Northern Apennines: sampling and processing methods. *Engineering Geology* **69**(1–2): 83–97.
- Chadwick OA, Derry LA, Vitousek PM, Huebert BJ, Hedin LO. 1999. Changing sources of nutrients during four million years of ecosystem development. *Nature* **397**(6719): 491–497.
- Chatanantavet P, Lajeunesse E, Parker G, Malverti L, Meunier P. 2010. Physically based model of downstream fining in bedrock streams with lateral input. *Water Resources Research* **46**(2): >W02518>. <https://doi.org/10.1029/2008WR007208>
- Clarke BA, Burbank DW. 2010. Bedrock fracturing, threshold hillslopes, and limits to the magnitude of bedrock landslides. *Earth and Planetary Science Letters* **297**(3–4): 577–586.
- Cui Y, Parker G. 2005. Numerical model of sediment pulses and sediment-supply disturbances in mountain rivers. *Journal of Hydraulic Engineering* **131**(8): 646–656.
- DiBiase RA, Rossi MW, Neely AB. 2018. Fracture density and grain size controls on the relief structure of bedrock landscapes. *Geology* **46**(5): 399–402.
- Dietrich WE, Kirchner JW, Ikeda H, Iseya F. 1989. Sediment supply and the development of the coarse surface layer in gravel-bedded rivers. *Nature* **340**(6230): 215–217.
- Dingle EH, Attal M, Sinclair HD. 2017. Abrasion-set limits on Himalayan gravel flux. *Nature* **544**(7651): 471–474.
- Fedele JJ, Paola C. 2007. Similarity solutions for fluvial sediment fining by selective deposition. *Journal of Geophysical Research – Earth Surface* **112**(F2): F02038. <https://doi.org/10.1029/2005JF000409>
- Ferguson R. 2003. The missing dimension: effects of lateral variation on 1-D calculations of fluvial bedload transport. *Geomorphology* **56**(1–2): 1–14.
- Ferguson R, Church M. 2009. A critical perspective on 1-D modeling of river processes: gravel load and aggradation in lower Fraser River. *Water Resources Research* **45**(11): W11424. <https://doi.org/10.1029/2009WR007740>
- Ferguson R, Hoey T, Wathen S, Werritty A. 1996. Field evidence for rapid downstream fining of river gravels through selective transport. *Geology* **24**(2): 179–182.
- Ferguson RI, Church M, Rennie CD, Venditti JG. 2015. Reconstructing a sediment pulse: modeling the effect of placer mining on Fraser River, Canada. *Journal of Geophysical Research - Earth Surface* **120**(7): 1436–1454.
- Finnegan NJ, Klier RA, Johnstone S, Pfeiffer AM, Johnson K. 2017. Field evidence for the control of grain size and sediment supply on steady-state bedrock river channel slopes in a tectonically active setting. *Earth Surface Processes and Landforms* **42**(14): 2338–2349.
- Gomez B, Rosser BJ, Peacock DH, Hicks DM, Palmer JA. 2001. Downstream fining in a rapidly aggrading gravel bed river. *Water Resources Research* **37**(6): 1813–1823.
- Granger DE, Riebe CS, Kirchner JW, Finkel RC. 2001. Modulation of erosion on steep granitic slopes by boulder armoring, as revealed by cosmogenic 26Al and 10Be. *Earth and Planetary Science Letters* **186**(2): 269–281.
- Haddadchi A, Booker DJ, Measures RJ. 2018. Predicting river bed substrate cover proportions across New Zealand. *Catena* **163**: 130–146.
- Hassan MA, Egozi R, Parker G. 2006. Experiments on the effect of hydrograph characteristics on vertical grain sorting in gravel bed rivers. *Water Resources Research* **42**(9): W09408. <https://doi.org/10.1029/2005WR004707>
- Hirt WH. 2007. Petrology of the Mount Whitney Intrusive Suite, eastern Sierra Nevada, California: implications for the emplacement and differentiation of composite felsic intrusions. *Geological Society of America Bulletin* **119**(9–10): 1185–1200.
- Howard AD. 1980. Thresholds in river regimes. *Thresholds in Geomorphology* **22**: 227–258.
- Ibbeken H, Schleyer R. 1986. Photo-sieving: a method for grain-size analysis of coarse-grained, unconsolidated bedding surfaces. *Earth Surface Processes and Landforms* **11**(1): 59–77.
- Kodama Y. 1994. Downstream changes in the lithology and grain size of fluvial gravels, the Watarase River, Japan; evidence of the role of abrasion in downstream fining. *Journal of Sedimentary Research* **64**(1a): 68–75.
- Le K, Lee J, Owen LA, Finkel R. 2007. Late Quaternary slip rates along the Sierra Nevada frontal fault zone, California: slip partitioning across the western margin of the eastern California Shear Zone–Basin and Range Province. *Geological Society of America Bulletin* **119**(1–2): 240–256.
- Lebedeva MI, Brantley SL. 2013. Exploring geochemical controls on weathering and erosion of convex hillslopes: beyond the empirical regolith production function. *Earth Surface Processes and Landforms* **38**(15): 1793–1807.
- Lenzi MA, D'Agostino V, Billi P. 1999. Bedload transport in the instrumented catchment of the Rio Cordon: Part I: analysis of bedload records, conditions and threshold of bedload entrainment. *Catena* **36**(3): 171–190.
- Lohse KA, Dietrich WE. 2005. Contrasting effects of soil development on hydrological properties and flow paths. *Water Resources Research* **41**(12): W12419. <https://doi.org/10.1029/2004WR003403>
- Lukens CE, Riebe CS, Sklar LS, Shuster DL. 2016. Grain size bias in cosmogenic nuclide studies of stream sediment in steep terrain. *Journal of Geophysical Research – Earth Surface* **121**(5): 978–999.
- Lukens CE, Riebe CS, Sklar LS, Shuster DL. 2020. Sediment size and abrasion biases in detrital thermochronology. *Earth and Planetary Science Letters* **531**: 115929. <https://doi.org/10.1016/j.epsl.2019.115929>
- Mao L, Lenzi MA. 2007. Sediment mobility and bedload transport conditions in an alpine stream. *Hydrological Processes: An International Journal* **21**(14): 1882–1891.
- Mao L, Uyttendaele GP, Iroumé A, Lenzi MA. 2008. Field based analysis of sediment entrainment in two high gradient streams located in Alpine and Andine environments. *Geomorphology* **93**(3–4): 368–383.
- Marshall JA, Sklar LS. 2012. Mining soil databases for landscape-scale patterns in the abundance and size distribution of hillslope rock fragments. *Earth Surface Processes and Landforms* **37**(3): 287–300.
- Marshall JA, Roering JJ, Bartlein PJ, Gavin DG, Granger DE, Rempel AW, Praskiewicz SJ, Hales TC. 2015. Frost for the trees: did climate increase erosion in unglaciated landscapes during the late Pleistocene? *Science Advances* **1**(10): e1500715. <https://doi.org/10.1126/sciadv.1500715>
- Miller KL, Szabó T, Jerolmack DJ, Domokos G. 2014. Quantifying the significance of abrasion and selective transport for downstream fluvial grain size evolution. *Journal of Geophysical Research – Earth Surface* **119**(11): 2412–2429.
- Neely AB, DiBiase RA, Corbett LB, Bierman PR, Caffee MW. 2019. Bedrock fracture density controls on hillslope erodibility in steep, rocky landscapes with patchy soil cover, southern California, USA. *Earth and Planetary Science Letters* **522**: 186–197.
- Nelson PA, Venditti JG, Dietrich WE, Kirchner JW, Ikeda H, Iseya F, Sklar LS. 2009. Response of bed surface patchiness to reductions in sediment supply. *Journal of Geophysical Research – Earth Surface* **114**(F2): F02005. <https://doi.org/10.1029/2008JF001144>
- Paola C, Parker G, Seal R, Sinha SK, Southard JB, P. R. Wilcock PR. 1992. Downstream fining by selective deposition in a laboratory flume. *Science* **258**(5089): 1757–1760.
- Parker G, Klingeman PC. 1982. On why gravel bed streams are paved. *Water Resources Research* **18**(5): 1409–1423.
- Parker G, Toro-Escobar CM. 2002. Equal mobility of gravel in streams: the remains of the day. *Water Resources Research* **38**(11): 46–41.
- Pitlick J, Mueller ER, Segura C, Cress R, Torizzo M. 2008. Relation between flow, surface-layer armoring and sediment transport in gravel-bed rivers. *Earth Surface Processes and Landforms* **33**(8): 1192–1209.
- Pizzuto JE. 1995. Downstream fining in a network of gravel-bedded rivers. *Water Resources Research* **31**(3): 753–759.
- PRISM Climate Group. 2014. Oregon State University, <http://prism.oregonstate.edu>.
- Riebe CS, Kirchner JW, Finkel RC. 2004. Sharp decrease in long-term chemical weathering rates along an altitudinal transect. *Earth and Planetary Science Letters* **218**(3–4): 421–434.
- Riebe CS, Sklar LS, Overstreet BT, Wooster JK. 2014. Optimal reproduction in salmon spawning substrates linked to grain size and fish length. *Water Resources Research* **50**(2): 898–918.

- Riebe CS, Sklar LS, Lukens CE, Shuster DL. 2015. Climate and topography control the size and flux of sediment produced on steep mountain slopes. *Proceedings of the National Academy of Sciences* **112**(51): 15574–15579.
- Roda-Boluda DC, D'Arcy M, McDonald J, Whittaker AC. 2018. Lithological controls on hillslope sediment supply: insights from landslide activity and grain size distributions. *Earth Surface Processes and Landforms* **43**(5): 956–977.
- Roy SG, Tucker GE, Koons PO, Smith SM, Upton P. 2016. A fault runs through it: Modeling the influence of rock strength and grain-size distribution in a fault-damaged landscape. *Journal of Geophysical Research – Earth Surface* **121**(10): 1911–1930.
- Scott DN, Wohl EE. 2019. Bedrock fracture influences on geomorphic process and form across process domains and scales. *Earth Surface Processes and Landforms* **44**(1): 27–45.
- Sklar LS, Dietrich WE. 2004. A mechanistic model for river incision into bedrock by saltating bed load. *Water Resources Research* **40**(6): W06301. <https://doi.org/10.1029/2003WR002496>
- Sklar LS, Dietrich WE. 2006. The role of sediment in controlling steady-state bedrock channel slope: implications of the saltation–abrasion incision model. *Geomorphology* **82**(1–2): 58–83.
- Sklar LS, Dietrich WE, Foufoula-Georgiou E, Lashermes B, Bellugi D. 2006. Do gravel bed river size distributions record channel network structure? *Water Resources Research* **42**(6): W06D18. <https://doi.org/10.1029/2006WR005035>
- Sklar LS, Riebe CS, Lukens CE, Bellugi D. 2016. Catchment power and the joint distribution of elevation and travel distance to the outlet. *Earth Surface Dynamics* **4**(4): 799–818.
- Sklar LS, Riebe CS, Marshall JA, Genetti J, Leclerc S, Lukens C, Mercés V. 2017. The problem of predicting the size distribution of sediment supplied by hillslopes to rivers. *Geomorphology* **277**: 31–49.
- Stock GM, Ehlers TA, Farley KA. 2006. Where does sediment come from? Quantifying catchment erosion with detrital apatite (U-Th)/He thermochronometry. *Geology* **34**(9): 725–728.
- Thompson C, Croke J. 2013. Geomorphic effects, flood power, and channel competence of a catastrophic flood in confined and unconfined reaches of the upper Lockyer valley, southeast Queensland, Australia. *Geomorphology* **197**: 156–169.
- Turowski JM, Wyss CR, Beer AR. 2015. Grain size effects on energy delivery to the streambed and links to bedrock erosion. *Geophysical Research Letters* **42**(6): 1775–1780.
- Whittaker AC, Attal M, Allen PA. 2010. Characterising the origin, nature and fate of sediment exported from catchments perturbed by active tectonics. *Basin Research* **22**(6): 809–828.
- Wohl EE, Pearthree PP. 1991. Debris flows as geomorphic agents in the Huachuca Mountains of southeastern Arizona. *Geomorphology* **4**(3–4): 273–292.
- Wohl E, Bledsoe BP, Jacobson RB, Poff NL, Rathburn SL, Walters DM, Wilcox AC. 2015. The natural sediment regime in rivers: broadening the foundation for ecosystem management. *Bioscience* **65**(4): 358–371.
- Wohl E, Brierley G, Cadol D, Coulthard TJ, Covino T, Fryirs KA, Grant G, Hilton RG, Lane SN, Magilligan FJ, Meitzen KM, Passalacqua P, Poepple RE, Rathburn SL, Sklar LS. 2019. Connectivity as an emergent property of geomorphic systems. *Earth Surface Processes and Landforms* **44**(1): 4–26.
- Yoo K, Weinman B, Mudd SM, Hurst M, Attal M, Maher K. 2011. Evolution of hillslope soils: the geomorphic theater and the geochemical play. *Applied Geochemistry* **26**: S149–S153.

Supporting Information

Additional supporting information may be found online in the Supporting Information section at the end of the article.

Data S1. Data reported in the article.

Data S2. Model calculations.